Crystallographic Insight into the Mg2+ Coordination Mode and N(SO2CF3)2– Anion Conformation in Mg[N(SO2CF3)2]2 and Its Adducts

AUTHOR(S):

Veryasov, Gleb; Harinaga, Ukyo; Matsumoto, Kazuhiko; Hagiwara, Rika

CITATION:

Veryasov, Gleb ...[et al]. Crystallographic Insight into the Mg2+ Coordination Mode and N(SO2CF3)2– Anion Conformation in Mg[N(SO2CF3)2]2 and Its Adducts. European Journal of Inorganic Chemistry 2017, 2017(7): 1087-1099

ISSUE DATE:

2017-02-17

URL:

http://hdl.handle.net/2433/230516

Crystallographic insight into the Mg^{2+} coordination mode and $N(SO_2CF_3)_2^-$ anion conformation in $Mg[N(SO_2CF_3)_2]_2$ and its adducts

Gleb Veryasov, Ukyo Harinaga, Kazuhiko Matsumoto*, Rika Hagiwara*

Department of Fundamental Energy Science, Graduate School of Energy Science, Kyoto University

Sakyo-ku, Kyoto 606-8501, Japan

E-mail: k-matsumoto@energy.kyoto-u.ac.jp (Kazuhiko Matsumoto), hagiwara@energy.kyoto-u.ac.jp (Rika Hagiwara)

Website: http://www.echem.energy.kyoto-u.ac.jp/

Abstract

The structures of magnesium bis(trifluoromethylsulfonyl)amide ($Mg[TFSA]_2$) and its adduct forms, $-[Mg(L)_n][TFSA]_2-$ with common ligands (L) such as ethanol, ethyl acetate, and water, namely $[Mg(C_2H_5OH)_4][TFSA]_2$, $[Mg(C_2H_5OH)_6][TFSA]_2$, $[Mg(C_2H_5OOCCH_3)_2][TFSA]_2$, $[Mg(H_2O)_2][TFSA]_2$, and $[Mg(H_2O)_6][TFSA]_2(H_2O)_2$, were prepared and characterized by single-crystal X-ray diffraction and Raman spectroscopy. In every case, Mg^{2+} was octahedrally coordinated to six O atoms of $TFSA^-$ and/or the ligand. The crystal structure of $Mg[TFSA]_2$ indicated the presence of disordered *cis* (12%) and *trans* (82%) ligand anion conformers. $[Mg(C_2H_5OH)_4][TFSA]_2$ appeared to be a new example of a coordination compound in which the $TFSA^-$ anions adopt a *trans* conformation while bonded to the metal core. Crystallographic data allowed us to propose a scheme of stepwise σ-donor ligand coordination to the Mg^{2+} core in $Mg[TFSA]_2$ and $[Mg(L)_n][TFSA]_2$ salts. This scheme is consistent with the literature data and indicates that the conformation of $TFSA^-$ anions in $[Mg(L)_n][TFSA]_2$ depends on the number of ligands coordinated to the Mg^{2+} core, regardless of the ligand.

Introduction

Since the discovery of bis(trifluoromethylsulfonyl)amide in $Xe[(N(SO_2CF_3)_2]_2$ by Foropoulos and DesMarteau,[1] $N(SO_2CF_3)_2^-$ ($TFSA^-$) salts have been investigated by many research groups.[2] Nowadays, these salts have applications as electrolytes in secondary batteries [3] or fuel cells,[4] and as catalysts in Diels-Alder [5] and Friedel-Crafts reactions.[6]

Recently, $Mg[TFSA]_2$ received recognition as an electrolyte in Mg secondary batteries, which are interesting candidates for post Li-ion batteries due to their high specific capacities, low reduction potential, and the reasonable price of magnesium.[7] However, there is little information on the structure of these electrolytes. For instance, the first report of a Mg^{2+} coordination state in $Mg[TFSA]_2$-based electrolytes, investigated by computational modeling, appeared in 2015.[8] Our recent crystallographic and spectroscopic work revealed that Mg^{2+} in the $Mg[TFSA]_2$-acetonitrile system adopts a homoleptic octahedral coordination with six N atoms from acetonitrile molecules.[2n] To our knowledge, the crystal structure of pure $Mg[TFSA]_2$, which provides valuable insight into understanding the $Mg(L)_n^{2+}$ (L = ligand) entity in $Mg[TFSA]_2$-based electrolytes, is not known.

Aside from practical applications, $TFSA^-$ salts are interesting targets for structural investigation. $TFSA^-$ anions can interact with metal centers as bidentate ligands or can bridge several metal centers.[9] Cation–anion and fluorous interactions between CF_3 groups commonly contribute to the formation of hydrophilic and hydrophobic domains in the lattices of TFSA salts.[9-10]

In 1998, Johansson *et al*. predicted the existence of *trans* and *cis* conformations for $TFSA^-$ using *ab initio* calculations.[11] The difference between conformers consists in the relative positions of the CF_3 groups with respect to the S−N−S plane; in the *trans* conformation, these groups are located on opposite sides of the plane, while in the *cis* conformation, they are on

the same side. In the same year with the original computational work, crystallographic evidence of both conformers was obtained by Žák *et al*.[12] Further work has allowed the regularity of the $TFSA^-$ conformation in different lattices to be tracked. The *trans* conformer usually occurs in structures with weak cation–anion interactions, while the *cis* conformer occurs in structures where $TFSA^-$ is bound to a metal center.[9, 13] However, exceptions to these rules also exist, including several examples where the anion adopts a *trans* conformation while coordinated to the metal core;[9] for instance [Rb(dioxane)$_2$][TFSA],[14] [Rb(H_2O)][TFSA],[13] Zn[TFSA]$_2$,[6] Li[TFSA],[4b, 15] and (*p*-cymene)Ru[TFSA]$_2$.[3d] To our knowledge, there is only one example of a $TFSA^-$ anion adopting a *cis* conformation without contacting the metal center, found in a 1,3-dimethyimidazolium salt,[16] for which the authors suggested that the formation of polar (charged) and apolar (fluorous) sheets in the lattice leads to stabilization of this conformation.

In the present work, an approach to grow high-quality Mg[TFSA]$_2$ crystals was established, allowing its crystal structure to be determined for the first time. In order to identify a general trend regarding the coordination environment of Mg^{2+} and the conformation of $TFSA^-$ anions in different coordination compounds, a series of novel adducted forms of Mg[TFSA]$_2$, [Mg(L)$_n$][TFSA]$_2$ with oxygen-containing σ-donor ligands ([Mg($C_2H_5OOCH_3$)$_2$][TFSA]$_2$, [Mg(H_2O)$_2$][TFSA]$_2$, [Mg(C_2H_5OH)$_4$][TFSA]$_2$, and [Mg(C_2H_5OH)$_6$][TFSA]$_2$) were prepared and characterized by single-crystal X-ray diffraction. Although another salt obtained in this work, [Mg(H_2O)$_6$][TFSA]$_2$(H_2O)$_2$, has previously been reported,[9, 17] the low-temperature data collection identified a new phase for this compound, which is also discussed. A scheme for stepwise ligand attachment to Mg^{2+} in Mg[TFSA]$_2$ and [Mg(L)$_n$][TFSA]$_2$ is proposed on the basis of the crystallographic data acquired. Raman spectra acquired for the coordination

compounds prepared supplemented the discussion of $TFSA^-$ bonding strength in these compounds, in terms of "weakly-bonded" and "strongly-bonded" systems.

Results and discussion

General remarks

All crystals in this study appeared to be transparent and colorless, and are stable in air for a short (<5 min) time. Pure $Mg[TFSA]_2$ and its adduct forms, $[Mg(C_2H_5OOCCH_3)_2][TFSA]_2$, $[Mg(H_2O)_2][TFSA]_2$, $[Mg(C_2H_5OH)_4][TFSA]_2$, and $[Mg(C_2H_5OH)_6][TFSA]_2$, are hygroscopic, and their crystals decompose due to moisture consumption when exposed to air for longer times. Long exposure of all these salts to air or any other source of moisture led to the formation of $[Mg(H_2O)_6][TFSA]_2(H_2O)_2$ as the final product, suggesting that water displaces any other ligand. Both adducts containing ethanol are temperature-sensitive and readily melt when heated above room temperature.

$Mg[TFSA]_2$ sublimes at elevated temperatures under a static vacuum, giving needle crystals suitable for single-crystal X-ray diffraction. The presence of trace amounts of water in the ampoule used for sublimation led to the formation of thin plate-like $[Mg(H_2O)_2][TFSA]_2$. The octahydrate, $[Mg(H_2O)_6][TFSA]_2(H_2O)_2$, was found to be unstable under dry conditions at room temperature. Single crystals of this salt lose water in a stream of dry nitrogen at 25 °C, affording a powder. Powder X-ray diffraction analysis of the decomposition product of this hydrate gave a different diffraction pattern to that simulated for the dihydrate, $[Mg(H_2O)_2][TFSA]_2$.

Crystal structures

Crystallographic data and refinement results for the present crystal structures are provided in Table 1. Geometrical parameters related to the Mg^{2+} coordination environment and the $TFSA^-$ anions are summarized in Tables 2 and 3, respectively (see Tables S1−S11 in the Supporting Information for further details).

$TFSA^-$ anion geometry

There are two enantiomers of *trans*-conformers observed in crystal structures, which differ in the sign of the C−S−N−S torsion angles. The two C−S−N−S angles in the *cis* conformer always have similar absolute values with opposite signs, whereas those in *trans* conformers always have the same sign. When both C1−S1−N1−S2 and S1−N1−S2−C2 torsion angles have negative values, the conformer might be denoted as N-*trans*; it is denoted as P-*trans* when both are positive (all $TFSA^-$ anion conformers and the numbering scheme used herein are shown in Figure S1). These two conformers are enantiomers. Henderson *et al.* observed disordered P-*trans* and N-*trans* conformers in the asymmetric units of $[Et_4N][TFSA]$ (Et = ethyl) [18] and $[pyr_{12}][TFSA]$ [19] (pyr_{12} = *N*-ethyl-*N*-methylpyrrolidinium).

Rotation around the S–N bond provides mechanical flexibility, which has a plasticizing effect on the polymer electrolytes, making the system more conductive.[11] At the same time, the possibility of CF_3 group rotation around the S−C bond results in rotational isomers. The diversity of $TFSA^-$ geometries in different compounds makes them interesting subjects for structural investigations. Moreover, $TFSA^-$ conformations in ionic liquids provide valuable information about their structure and properties.[2g, 2i, 20] The following discussion of $Mg[TFSA]_2$ and $[Mg(L)_n][TFSA]_2$ crystal structures allowed us to identify new rules guiding the conformation of $TFSA^-$ in the solid state in this series of compounds.

Table 1. Crystal data and refinement results for $Mg[TFSA]_2$ and $[Mg(L)_n][TFSA]_2$ (L = $C_2H_5OOCCH_3$, C_2H_5OH and H_2O).

Compound	$Mg[TFSA]_2$	$[Mg(C_2H_5OOCCH_3)_2][TFSA]_2$	$[Mg(H_2O)_2][TFSA]_2$	$[Mg(C_2H_5OH)_4][TFSA]_2$	$[Mg(C_2H_5OH)_6][TFSA]_2$	$[Mg(H_2O)_6][TFSA]_2(H_2O)_2$
formula	$MgN_2S_4O_8C_4F_{12}$	$MgN_2S_4O_{12}C_{12}F_{12}H_{16}$	$MgN_2S_4O_{10}C_{12}F_{12}H_4$	$MgN_2S_4O_{12}C_{10}F_{12}H_{24}$	$MgN_2S_4O_{14}C_{14}F_{12}H_{36}$	$MgN_2S_4O_{16}C_4F_{12}H_{16}$
fw	768.88	760.82	620.64	768.88	861.02	728.74
T /K	173	113	113	113	113	113
cryst. system	monoclinic	monoclinic	monoclinic	monoclinic	monoclinic	monoclinic
space group	*C*2/*c*	*C*2	$P2_1/n$	*C*2/*c*	$P2_1/n$	$P2_1/n$
a / Å	19.481(2)	22.956(3)	18.5687(8)	14.9170(9)	9.0897(12)	12.6725(3)
b / Å	9.2358(11)	7.2425(9)	7.2547(4)	12.4584(9)	12.4471(16)	14.3964(3)
c / Å	9.6085(9)	19.870(3)	11.3048(6)	16.3409(11)	16.7166(17)	14.6487(4)
β / deg	96.118(3)	124.431(5)	38.419(2)	103.020(2)	92.756(3)	107.4210(10)
V/ Å^3	1719.0(3)	2724.8(6)	946.33(9)	2958.8(3)	1889.1(4)	2549.90(11)
Z	4	4	2	4	2	4
ρ_{calc} / g cm^{-3}	1.726	1.855	2.178	1.726	1.514	1.898
μ / mm^{-1}	0.76	0.51	0.70	0.47	0.38	0.55
F(000)	1144	1528	612	1560	884	1464
θ range, °	3.2-27.5	3.0-27.5	3.3-27.5	3.1-27.5	3.1-24.3	3.2-27.5
reflns. collect	8139	6725	8888	14024	13143	24455
reflns. indep.	1957	4695	2175	3370	3042	5812
reflns (I>2σ)	1183	4345	1989	3017	2523	5424
R_1[a]	0.053	0.037	0.033	0.050	0.055	0.025
wR_2[b]	0.153	0.130	0.085	0.121	0.150	0.069
GoF on F^2	1.04	1.11	1.06	1.07	1.04	0.92
cryst. size/ mm^3	0.15 x 0.30 x 0.35	0.50 × 0.25 × 0.20	0.30 × 0.20 × 0.10	0.50 x 0.30 x 0.30	0.60 × 0.40 × 0.40	0.50 x 0.40 x 0.40
CCDC	1486816	1486819	1486815	1486817	1486818	1486820

[a] $R_1 = \Sigma||F_o| - |F_c|| / \Sigma|F_o|$
[b] $R_2 = [\Sigma w(F_o^2 - F_c^2)^2 / \Sigma w(F_o^2)^2]^{1/2}$

$Mg[TFSA]_2$

Utilizing sublimation as a convenient technique for the purification of metal $TFSA^-$ salts was first reported by Earle *et al.*[6, 21] In the present work, $Mg[TFSA]_2$ was sublimed under static vacuum in a sealed ampoule. Heating at 300 °C for 20 h resulted in the formation of high-quality colorless needles. The $Mg[TFSA]_2$ crystals were extremely sensitive to moisture and the presence of any σ-donor ligands. Prolonged exposure to a dry air atmosphere (water content <10 ppm) led to $Mg[TFSA]_2$ crystal cleavage due to moisture uptake.

The asymmetric unit determined at –160 °C contained a pair of Mg^{2+} and $TFSA^-$ ions, (Figure 1; some atom labels are omitted for clarity). The peculiar disorder of the anion was unique to this structure. The part marked "a" corresponds to the *trans* conformation, and "b" the *cis* conformation. To our knowledge, this is the first example of a compound containing both conformers of $TFSA^-$ in a disordered manner, sharing the same position in the crystal lattice. The mode of disorder could be best described as follows. The CF_3SO_2N group of the anion, containing C1 and S1 atoms, is fixed, with the remaining SO_2CF_3 group, containing S2 and C2 atoms, adopting two positions that differ in the relative position of CF_3 with respect to the plane of Mg1, S1, and N1 atoms. The fractions of *trans* and *cis* were determined to be 82% and 18%, respectively, from the crystallographic data and were essentially unchanged in all crystals examined, despite being picked from different batches. This ratio was also unaffected by temperature; crystals recorded at −120 °C and −10 °C had a constant ratio of *trans* to *cis* conformers, with a deviation of ±1%.

The Mg^{2+} ion had an octahedral environment and formed bonds with four $TFSA^-$ anions. Each anion contacted two Mg^{2+} ions, as shown in Figure 2 (some parts of the $TFSA^-$ anions are omitted for clarity). It should be noted that O4 (O4a ad O4b), which occupied different positions in the *cis* and *trans* conformers, did not participate in the formation of Mg···O

interactions. This might have caused the conformational freedom in this structure. The Mg···O distances for two bonds formed with the same anion were 2.072(3) Å and 2.046(11) Å (Mg···O2 and Mg···O3a, respectively) for the *trans* conformer and 2.072(3) Å and 1.97(6) Å (Mg···O2 and Mg···O3b, respectively) for the *cis* conformer. The Mg···O1 bond was slightly longer than the others and had a value of 2.090(3) Å. The O···Mg···O angles deviated 90° from the ideal octahedron and, of particular note, the O3b···Mg1···O2 had a value of 83.5(18)°. All bond lengths and angles for the Mg^{2+} coordination environment are listed in Table 2.

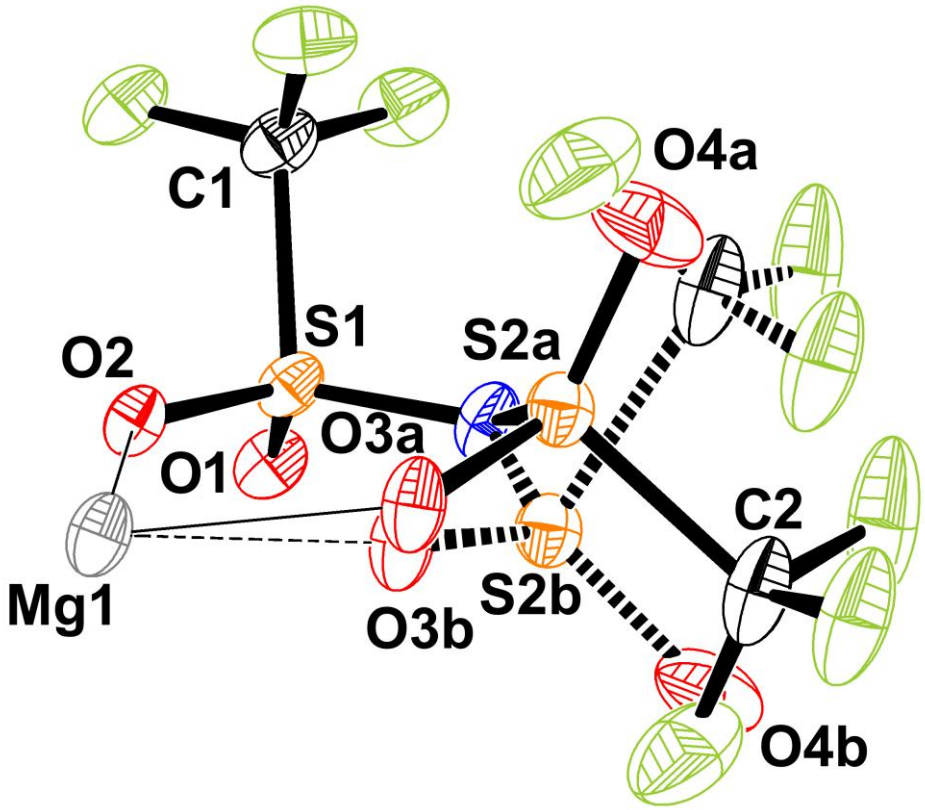

Figure 1. The asymmetric unit of the $Mg[TFSA]_2$ crystal structure determined at −160 °C. Thermal ellipsoids are drawn at the 30% probability level.

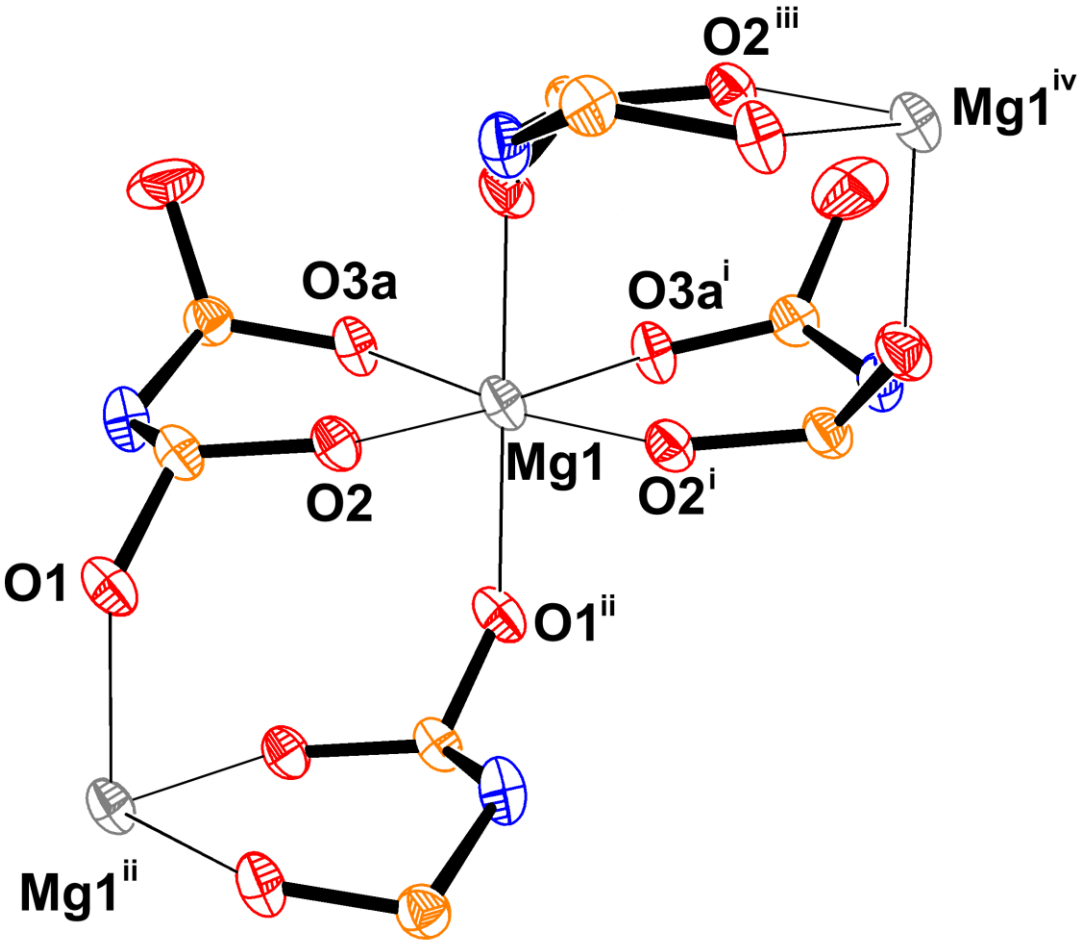

Figure 2. The octahedral surrounding of Mg^{2+} in $Mg[TFSA]_2$. The *cis*-conformer is omitted for clarity. Thermal ellipsoids are drawn at the 30% probability level (symmetry codes: (i) 1–*x*; *y*; 1/2–*z*; (ii) 1–*x*, –*y*, 1–*z*; (iii) *x*, –*y*, –1/2; (iv) 1–*x*, –*y*, –*z*).

Table 2. Geometrical parameters of Mg···O interactions (Å, °) in $Mg[TFSA]_2$ and its adducts containing $C_2H_5OOCCH_3$, C_2H_5OH, and H_2O.

$Mg(TFSA)_2$											
Mg1···O3b^{i}	1.97 (6)	Mg1—O1^{ii}	2.090 (3)	O3a^{i}—Mg1—O2	174.99 (18)	O2—Mg1—O2^{i}	95.27 (16)	O2^{i}—Mg1—O1^{ii}	88.72 (11)	O2^{i}—Mg1—O1^{iii}	87.85 (11)
Mg1—O3b	1.97 (6)	Mg1—O1^{iii}	2.090 (3)	O3a—Mg1—O2	86.8 (3)	O3b^{i}—Mg1—O1^{ii}	96.8 (16)	O3b^{i}—Mg1—O1^{iii}	86.6 (15)	O1^{ii}—Mg1—O1^{iii}	174.90 (19)
Mg1—O3a^{i}	2.046 (11)	O3b^{i}—Mg1—O3b	98 (3)	O3b^{i}—Mg1—O2^{i}	83.5 (18)	O3b—Mg1—O1^{ii}	86.6 (15)	O3b—Mg1—O1^{iii}	96.8 (16)		
Mg1—O3a	2.046 (11)	O3a^{i}—Mg1—O3a	91.4 (6)	O3b—Mg1—O2^{i}	175.2 (13)	O3a^{i}—Mg1—O1^{ii}	87.7 (2)	O3a^{i}—Mg1—O1^{iii}	95.9 (2)		
Mg1—O2	2.072 (3)	O3b^{i}—Mg1—O2	175.2 (13)	O3a^{i}—Mg1—O2^{i}	86.8 (3)	O3a—Mg1—O1^{ii}	95.9 (2)	O3a—Mg1—O1^{iii}	87.7 (2)		
Mg1—O2^{i}	2.072 (3)	O3b—Mg1—O2	83.5 (18)	O3a—Mg1—O2^{i}	174.99 (18)	O2—Mg1—O1^{ii}	87.85 (11)	O2—Mg1—O1^{iii}	88.72 (11)		
Symmetry codes: (i) −x+1, y, −z+1/2; (ii) −x+1, −y, −z+1; (iii) x, −y, z−1/2.											
$[Mg(C_2H_5OOCCH_3)_2][TFSA]_2$											
Mg1—O16^{i}	2.011 (3)	Mg2—O7^{iv}	2.081 (3)	O16^{i}—Mg1—O16	173.6 (2)	O16^{i}—Mg1—O2^{i}	88.88 (11)	O3^{ii}—Mg1—O2	175.92 (12)	O26—Mg2—O6^{vi}	89.60 (14)
Mg1—O16	2.011 (3)	Mg2—O26^{iv}	1.979 (3)	O16^{i}—Mg1—O3^{ii}	90.42 (11)	O16—Mg1—O2^{i}	86.76 (11)	O3^{iii}—Mg1—O2	88.89 (10)	O26^{iv}—Mg2—O6^{vi}	94.02 (14)
Mg1—O3^{ii}	2.068 (3)	Mg2—O6^{v}	2.069 (3)	O16—Mg1—O3^{ii}	94.17 (11)	O3^{ii}—Mg1—O2^{i}	88.89 (10)	O2^{i}—Mg1—O2	93.99 (17)	O6^{v}—Mg2—O6^{vi}	88.28 (18)
Mg1—O3^{iii}	2.068 (3)	Mg2—O6^{vi}	2.069 (3)	O16^{i}—Mg1—O3^{iii}	94.17 (11)	O3^{iii}—Mg1—O2^{i}	175.92 (12)	O26—Mg2—O26^{iv}	175.0 (3)	O26—Mg2—O7	89.65 (14)
Mg1—O2^{i}	2.075 (3)	Mg2—O7	2.081 (3)	O16—Mg1—O3^{iii}	90.42 (11)	O16^{i}—Mg1—O2	86.76 (11)	O26—Mg2—O6^{v}	94.02 (14)	O26^{iv}—Mg2—O7	86.92 (14)
Mg1—O2	2.075 (3)	O6^{v}—Mg2—O7^{iv}	88.89 (12)	O3^{ii}—Mg1—O3^{iii}	88.38 (16)	O16—Mg1—O2	88.88 (11)	O26^{iv}—Mg2—O6^{v}	89.60 (14)	O6^{v}—Mg2—O7	175.36 (13)
Mg2—O26	1.979 (3)	O6^{vi}—Mg2—O7^{iv}	175.36 (13)	O6^{vi}—Mg2—O7	88.89 (12)	O26—Mg2—O7^{iv}	86.92 (13)	O26^{iv}—Mg2—O7^{iv}	89.65 (14)	O7—Mg2—O7^{iv}	94.15 (19)
Symmetry codes: (i) −x+2, y, −z+1; (ii) −x+2, y−1, −z+1; (iii) x, y−1, z; (iv) −x+2, y, −z+2; (v) −x+2, y+1, −z+2; (vi) x,y+1, z.											
$[Mg(H_2O)_2][TFSA]_2$											
Mg1—O5^{i}	2.0232 (13)	Mg1—O2^{iii}	2.0802 (12)	O5^{i}—Mg1—O5	180.0	O5^{i}—Mg1—O3	92.53 (5)	O5^{i}—Mg1—O2^{ii}	90.27 (5)	O3—Mg1—O2^{ii}	87.80 (5)
Mg1—O5	2.0232 (13)	Mg1—O3	2.0630 (12)	O5^{i}—Mg1—O3^{i}	87.47 (5)	O5—Mg1—O3	87.47 (5)	O5—Mg1—O2^{ii}	89.73 (5)		
Mg1—O3^{i}	2.0630 (12)	O5^{i}—Mg1—O2^{iii}	89.73 (5)	O5—Mg1—O3^{i}	92.53 (5)	O3^{i}—Mg1—O3	180.0	O3^{i}—Mg1—O2^{ii}	92.20 (5)		
Mg1—O2^{ii}	2.0802 (12)	O5—Mg1—O2^{iii}	90.27 (5)	O3^{i}—Mg1—O2^{iii}	87.80 (5)	O3—Mg1—O2^{iii}	92.20 (5)	O2^{ii}—Mg1—O2^{iii}	180.0		
Symmetry codes: (i) −x−1, −y+1, −z+3; (ii) −x−1, −y, −z+3; (iii) x, y+1, z.											
$[Mg(C_2H_5OH)_4][TFSA]_2$											
Mg1—O5	2.042 (2)	Mg1—O4	2.073 (2)	O5—Mg1—O5^{i}	175.52 (15)	O5—Mg1—O6	94.61 (9)	O5—Mg1—O4	91.44 (9)	O6—Mg1—O4	173.95 (9)
Mg1—O5^{i}	2.042 (2)	Mg1—O4^{i}	2.073 (2)	O5—Mg1—O6^{i}	88.51 (9)	O5^{i}—Mg1—O6	88.51 (9)	O5^{i}—Mg1—O4	85.44 (9)		
Mg1—O6^{i}	2.046 (2)	O5—Mg1—O4^{i}	85.44 (9)	O5^{i}—Mg1—O6^{i}	94.61 (9)	O6^{i}—Mg1—O6	91.78 (15)	O6^{i}—Mg1—O4	88.57 (9)		
Mg1—O6	2.046 (2)	O5^{i}—Mg1—O4^{i}	91.44 (9)	O6^{i}—Mg1—O4^{i}	173.95 (9)	O6—Mg1—O4^{i}	88.57 (9)	O4—Mg1—O4^{i}	91.72 (13)		
Symmetry code: (i) −x, y, −z+1/2.											
$[Mg(C_2H_5OH)_6][TFSA]_2$											
Mg1—O11	2.045 (2)	Mg1—O14^{i}	2.064 (2)	O11—Mg1—O11^{i}	180.00 (7)	O11—Mg1—O17	92.57 (10)	O11—Mg1—O14^{i}	87.16 (11)	O17—Mg1—O14^{i}	86.47 (11)
Mg1—O11^{i}	2.045 (2)	Mg1—O14	2.064 (2)	O11—Mg1—O17^{i}	87.43 (10)	O11^{i}—Mg1—O17	87.43 (10)	O11^{i}—Mg1—O14^{i}	92.84 (11)		
Mg1—O17^{i}	2.061 (2)	O11—Mg1—O14	92.84 (11)	O11^{i}—Mg1—O17^{i}	92.57 (10)	O17^{i}—Mg1—O17	180.00 (8)	O17^{i}—Mg1—O14^{i}	93.53 (11)		
Mg1—O17	2.061 (2)	O11^{i}—Mg1—O14	87.16 (11)	O17^{i}—Mg1—O14	86.47 (11)	O17—Mg1—O14	93.53 (11)	O14^{i}—Mg1—O14	180.00 (11)		
Symmetry codes: (i) −x+1, −y+1, −z+1.											
$[Mg(H_2O)_6][TFSA]_2(H_2O)_2$											
Mg1—O4	2.0410 (10)	Mg1—O2	2.0598 (10)	O4—Mg1—O5	90.18 (4)	O4—Mg1—O3	86.98 (4)	O4—Mg1—O2	178.19 (4)	O3—Mg1—O2	91.26 (4)
Mg1—O5	2.0428 (10)	Mg1—O1	2.0642 (10)	O4—Mg1—O6	91.37 (4)	O5—Mg1—O3	91.45 (4)	O5—Mg1—O2	89.44 (4)		
Mg1—O6	2.0554 (10)	O4—Mg1—O1	90.90 (4)	O5—Mg1—O6	178.33 (4)	O6—Mg1—O3	89.26 (4)	O6—Mg1—O2	89.03 (4)		
Mg1—O3	2.0563 (10)	O5—Mg1—O1	87.35 (4)	O6—Mg1—O1	92.00 (4)	O3—Mg1—O1	177.56 (4)	O2—Mg1—O1	90.85 (4)		

The C−S···S−C torsion angle in $TFSA^-$, which has been used frequently for the discussion of $TFSA^-$ geometries,[20a] had values of −134.2(3)° (C1−S1···S2a−C2a) in the *trans* conformer and −3.8(7)° (C1−S1···S2b−C2b) in the *cis* conformer. The geometry was significantly distorted from that of the stationary point obtained in a previous computational study, which predicted the torsion angle to be approximately 170° for *trans* and 30−70° for *cis* conformers.[20a] Presumably, this difference was caused by interaction with the small Mg^{2+} and repulsion between neighboring anions.

The packing for $Mg[TFSA]_2$ is shown in Figure 3; the *cis* conformers of the anion are omitted for clarity. The packing diagram for $Mg[TFSA]_2$ containing only *cis* conformers of $TFSA^-$ is shown in Figure S2. The lattice consists of 1D chains oriented along the crystallographic *c* axis and organized in 2D layers. Formation of the layered structure containing fluorous apolar domains has been commonly observed in alkali and alkali earth metal $TFSA^-$ salts [4b, 9, 13, 22] as well as in trifluoromethylsulfonates and fluorosulfates. [23]

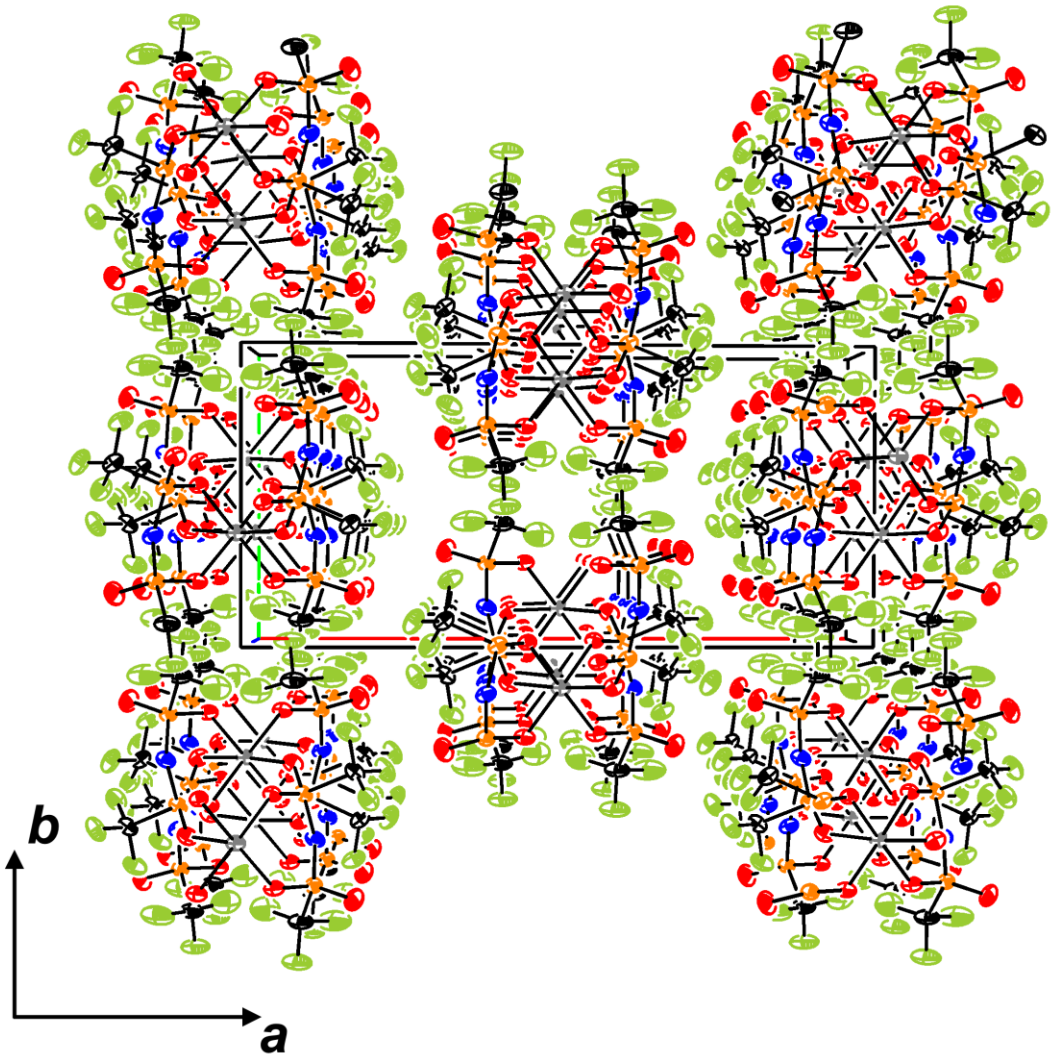

Figure 3. Packing diagram for $Mg[TFSA]_2$ along the *c* axis. Thermal ellipsoids are given at the 30% probability level. Disordered part containing *cis* conformers of $TFSA^-$ is omitted for clarity.

The powder XRD patterns of dry $Mg[TFSA]_2$ powder at three different temperatures, 25, 145, and 180 °C, resembled each other and were in good agreement with the simulated pattern of the present $Mg[TFSA]_2$ structure at –160 °C, suggesting that no significant phase transition occurred in $Mg[TFSA]_2$ within this temperature range (see Figure S3). It should be noted that a wet $Mg[TFSA]_2$ sample produced endothermic peaks during the heating scan in DSC that

originated from the hydrates (see Figure S4). The DSC patterns of the same sample kept under dynamic vacuum at 200 °C for 5 h and 15 h appeared to be completely different, with the most intense endothermic peaks disappearing from the sample dried for longer. Presumably, the peaks at around 100 °C were due to the residual hydrates. These peaks could be erroneously considered as those for phase transitions of $Mg[TFSA]_2$.

Table 3. Geometrical parameters (Å,°) of $TFSA^-$ anions in $Mg[TFSA]_2$, $[Mg(C_2H_5OOCCH_3)_2][TFSA]$, $[Mg(H_2O)_2][TFSA]_2$, $[Mg(C_2H_5OH)_4][TFSA]_2$, $[Mg(C_2H_5OH)_6][TFSA]_2$, $[Mg(H_2O)_6][TFSA]_2(H_2O)_2$, and related compounds [a]

Compound, anion conformation	C1−S1	S1−N1	N1−S2	S2−C2	C1−S1−N1−S2	S1−N1−S2−C2	C1−S1···S2−C2	Source
$Mg[TFSA]_2$, *trans*	1.833(5)	1.546(3)	1.629(4)	1.817(6)	150.4(3)	88.2(3)	-134.2(3)	T*
$Mg[TFSA]_2$, *cis*	1.833(5)	1.546(3)	1.478(7)	2.01(5)	128.9(5)	–125.4(6)	–3.8(7)	T*
$[Mg(C_2H_5OOCCH_3)_2][TFSA]_2$, *cis*	1.842(4) 1.832(4)	1.569(3) 1.562(4)	1.554(3) 1.561(4)	1.853(4) 1.829(5)	112.5(3) 105.0(3)	–113.1(3) –109.1(3)	–0.5(3) –4.1(3)	T*
$[Mg(H_2O)_2][TFSA]_2$, *cis*	1.8411(19)	1.5671(14)	1.5559(14)	1.8370(19)	–115.02(13)	109.51(13)	4.92(10)	T*
$[Mg(C_2H_5OH)_4][TFSA]_2$, *trans*	1.832(3)	1.576(2)	1.567(2)	1.823(3)	–102.5(2)	–98.7(2)	–173.15(16)	T*
$[Mg(C_2H_5OH)_6][TFSA]_2$, *trans*	1.812(5)	1.570(3)	1.563(3)	1.835(4)	–103.5(3)	–90.6(3)	179.8(3)	T*
$[Mg(H_2O)_6][TFSA]_2(H_2O)_2$, *trans*	1.8325(15) 1.8404(14)	1.5780(11) 1.5840(11)	1.5878(11) 1.5857(11)	1.8378(14) 1.8338(16)	91.94(9) 87.63(9)	92.66(9) 100.43(10)	171.75(7) 174.62(7)	T*
Li[TFSA], *trans*	1.901	1.557	1.557	1.901	–92.7	–92.7	–171.71	Ref [4b]
$Zn[TFSA]_2$, *trans*	1.835	1.567	1.531	1.833	101.7	138.9	133.29	Ref [6]
$[Rb(dioxane)_2][TFSA]$, *trans*	1.814	1.550	1.563	1.803	113.7	110.9	147.24	Ref [14]
$[Rb(H_2O)][TFSA]$, *trans*	1.834	1.576	1.572	1.831	98.3	86.8	172.65	Ref [13]
$[Mg(CH_3CN)_6][TFSA]_2$, *trans*	1.8266	1.5809	1.5702	1.8294	109.27	94.10	169.32	Ref [2n]

[a] See Figure S1 in the Supporting Information for atom numbering scheme; T* = this work.

$[Mg(C_2H_5OOCCH_3)_2][TFSA]_2$ and $[Mg(H_2O)_2][TFSA]_2$

$[Mg(C_2H_5OOCCH_3)_2][TFSA]_2$ salt was prepared from an ethyl acetate solution of $Mg[TFSA]_2$. The system was extremely sensitive to moisture, and using magnesium salt or solvent with trace amounts of water made crystallization impossible due to the formation of hydrates. $[Mg(H_2O)_2][TFSA]_2$ salt was obtained by coordination with trace water during an attempt to prepare pure $Mg[TFSA]_2$ crystals from dichloromethane in an autoclave.

These two compounds had similar structures, rendering 1D chains in which two Mg^{2+} cations were double-bridged by two $TFSA^-$ anions, with the four equatorial positions of the octahedron coordinated to O atoms from different $TFSA^-$ anions, as shown in Figure 4. Ligand oxygen atoms were located in the two axial positions of the octahedron in *trans*, out of the planes involving Mg^{2+} cations and the O atoms in the $TFSA^-$ anions. The asymmetric unit of $[Mg(C_2H_5OOCCH_3)_2][TFSA]_2$ contained two crystallographically independent Mg^{2+} (Mg1 and Mg2) ions, belonging to two different chains, two $TFSA^-$ anions, and two ethyl acetate molecules (see Figure S5); the chains in the lattice contain exclusively Mg1 or Mg2. Although both ethyl acetate molecules are disordered (see Figure S6 for a clear representation), reflecting their positional freedom in the crystal lattice, the carbonyl O atoms interacting with Mg^{2+} (O16 and O26) were fixed and ordered.

The Mg···O distances for $TFSA^-$ were comparable in both compounds, and fell into the range of 2.068(3)–2.081(3) Å for $[Mg(C_2H_5OOCCH_3)_2][TFSA]_2$, and 2.0630(12)–2.0802(12) Å for $[Mg(H_2O)_2][TFSA]_2$. The Mg···O distances for the water or ethyl acetate molecules were shorter than those for the $TFSA^-$ anions (see Tables 2 and S2) and in $[Mg(C_2H_5OOCCH_3)_2][TFSA]_2$ they have values of 1.979(3) and 2.011(3) Å for Mg1···O16 and Mg2···O26 (Mg2 and O26 belong to another chain in the asymmetric unit), respectively, and were slightly longer than that previously reported, 2.053(4) Å in

$[Mg(C_2H_5OOCCH_3)_6][AlCl_4]_2$.[24] In $[Mg(H_2O)_2][TFSA]_2$, the Mg1···O5 distance was 2.0232(13) Å. The *cis* O···Mg···O angles in the chain fell within the range 88.38(16)° ($O3^{ii}$···Mg2···$O3^{iii}$)–93.99(17)° ($O2^{i}$···Mg1···O2) in $[Mg(C_2H_5OOCCH_3)_2][TFSA]_2$, and had a value of 92.20(5)° (O3···Mg1···$O2^{iii}$) in $[Mg(H_2O)_2][TFSA]_2$. The $TFSA^-$ anions in both structures adopted *cis* conformations, as is common for strongly-bonded bidentate anions.[9].

The packing diagrams for both compounds are shown in Figure 5. Hydrogen atoms in the $[Mg(C_2H_5OOCCH_3)_2][TFSA]_2$ structure are omitted for clarity. In both cases, 1D chains are oriented along the crystallographic *b* axis. The CF_3 groups form apolar columns in $[Mg(C_2H_5OOCCH_3)_2][TFSA]_2$ and apolar layers in $[Mg(H_2O)_2][TFSA]_2$. The packing mode of $[Mg(H_2O)_2][TFSA]_2$ could be described as 2D layers composed of 1D chains.

It is important to note that *D*–H···A (*D*, donor; H, hydrogen; A, acceptor) interactions below the van der Waals radii were only present in $[Mg(C_2H_5OOCCH_3)_2][TFSA]_2$ inside the chains, with no *D*–H···A contacts between neighboring chains. This observation allowed us to conclude that the 1D chains were interconnected exclusively by hydrophobic interactions, similar to chains in the previously reported $Zn[TFSA]_2$[6] structure or the $Mg[TFSA]_2$ structure in the present work. There were only two *D*–H···A contacts in the $[Mg(C_2H_5OOCCH_3)_2][TFSA]_2$ structure, C11a–H11d···O1 and C21a–H21c···O8 (or C11b–H11a···O1 and C21b–H21f···O8 for another chain), between the unbound O atom of $TFSA^-$ and methyl group of ethyl acetate (see Table S4). Presumably, the absence of strong *D*–H···A interactions contributed to the disorder of ethyl acetate molecules. There are three contacts between hydrogen atoms and unbound O atoms of $TFSA^-$ in the $[Mg(H_2O)_2][TFSA]_2$ structure (see Table S5 and Figure S7). O5–H2···$O4^{iii}$ contact occurred with oxygen from the anion in the same chain, while O5–H2···$O1^{ii}$ and O5–H1···$O4^{i}$ occurred between two neighboring chains.

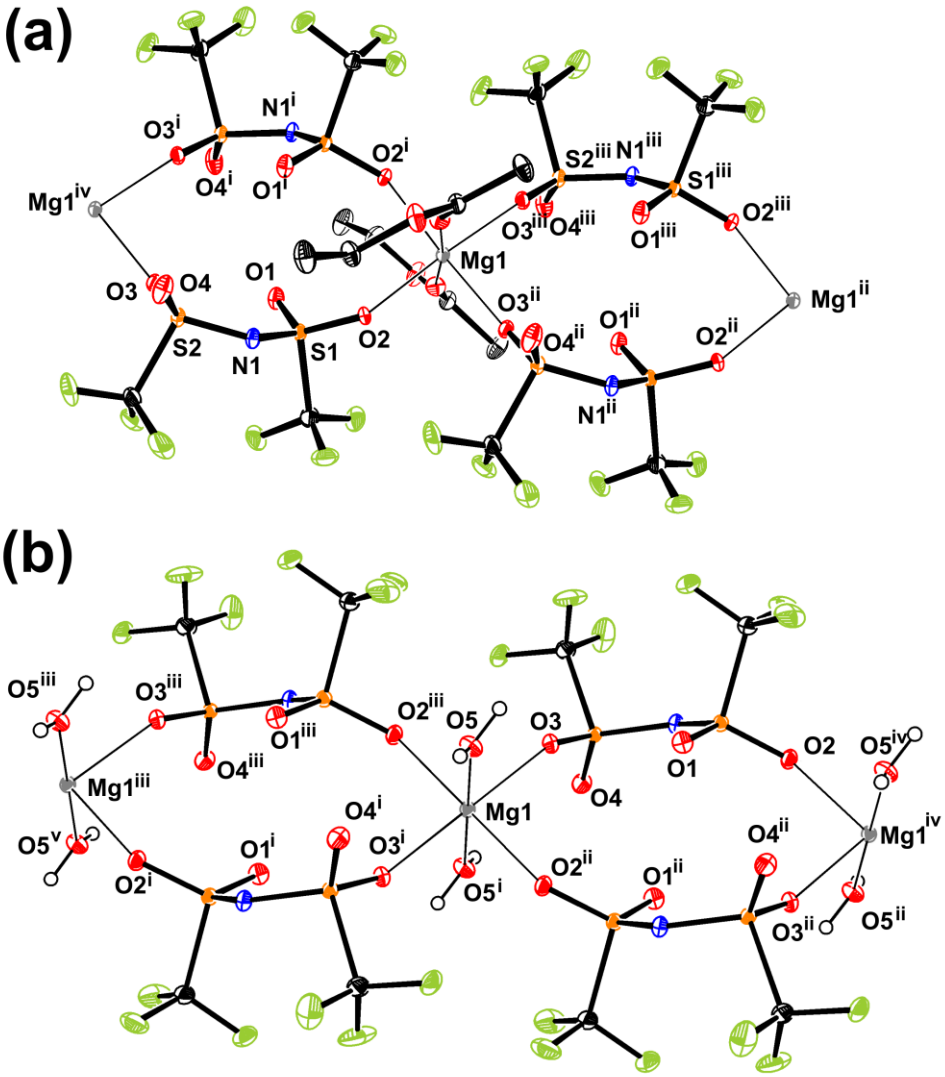

Figure 4. 1D chains in the structures of (a) $[Mg(C_2H_5OOCCH_3)_2][TFSA]_2$ (ethylacetate disorder is omitted for clarity) and (b) $[Mg(H_2O)_2][TFSA]_2$. Thermal ellipsoids are given at the 30% probability level. Hydrogen atoms in the ethyl acetate ligands are omitted for clarity (symmetry codes for (a): (i) *–x*, *y*, *–z*, (ii) *x*, *y*–1, *z* (iii) *–x*, *y*–1, *–z* (iv) *x*, 1+*y*, *z*; symmetry

codes for (b): (i) −1−*x*, −*y*+1, −*z*+3; (ii) −1−*x*, −*y*, −*z*+3; (iii) *x*, *y*+1, *z*; (iv) *x*, *y*−1, *z* (v) −1−*x*, 2−*y*, −*z*+3).

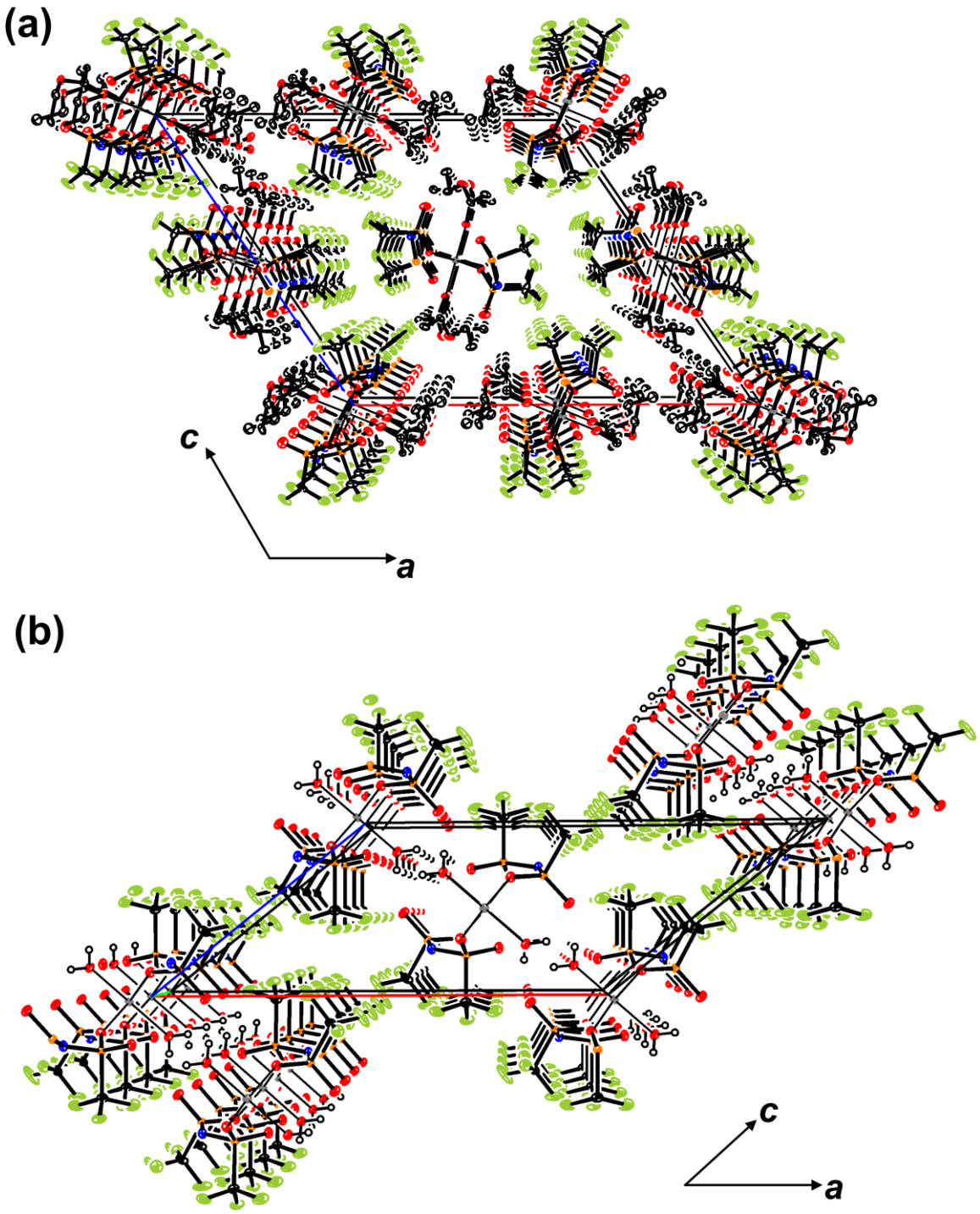

Figure 5. Packing diagrams for (a) $[Mg(C_2H_5OOCCH_3)_2][TFSA]_2$ and (b) $[Mg(H_2O)_2][TFSA]_2$. Thermal ellipsoids are given at the 30% probability level.

$[Mg(C_2H_5OH)_4][TFSA]_2$

Although the first discovery of $[Mg(C_2H_5OH)_4][TFSA]_2$ formation was serendipitous, it was repeatedly prepared using the technique described in the experimental section. The compound appeared to have a melting point slightly above room temperature and crystals had to be manipulated in a cold place.

The coordination environment of Mg^{2+} in $[Mg(C_2H_5OH)_4][TFSA]_2$ is shown in Figure 6. The Mg^{2+} ion has an octahedral structure surrounded by six O atoms from four ethanol molecules and two $TFSA^-$ anions, with the anions situated in *cis* positions in the octahedral arrangement of O atoms around Mg atoms. The Mg···O bond lengths for the ethanol molecules (2.042(2) and 2.046(2) Å) were slightly shorter than those with $TFSA^-$ (2.073(2) Å). The O4···Mg1···O42^{i} angle formed with oxygen atoms from two $TFSA^-$ ligand anions was 91.72(13), whereas the O···Mg1···O angles formed with oxygen atoms from two ethanol ligands in *cis* positions in the Mg^{2+} coordination octahedra varied from 85.44(9)° for O5^{i}···Mg1···O4 to 94.61(9)° for O5···Mg1···O6 (see Table S6 for more details).

One of the most intriguing and unusual features of this structure was the *trans* conformation of the $TFSA^-$ anion when bound to the metal core (see Table 3 for details). Each $TFSA^-$ anion was connected to only one Mg^{2+} through an Mg···O bond. In all previously known compounds, $TFSA^-$ anions were connected to at least two (in $Zn[TFSA]_2$[6]) and up to five (in $Rb[TFSA]\cdot H_2O$[13]) different metal cores, with no examples of *trans* $TFSA^-$ bound to one metal core. It is noteworthy that the bis(methylsulfonyl)amide anion (MSA^-, $(CH_3SO_2)_2N^-$), which has a molecular structure similar to $TFSA^-$, has adopted a *trans* conformation in

several tetrahydrates, $[M(H_2O)_4][MSA]_2$ (M = Mg, Ni, Cu, and Zn), although it is bonded to the metal core.[25] To our knowledge, there are no known analogous tetrahydrates with $TFSA^-$ anions. The coordination structure around Mg^{2+} in $[Mg(C_2H_5OH)_4][TFSA]_2$ was similar to that of $[Mg(H_2O)_4][MSA]_2$.[25]

The packing diagram for $[Mg(C_2H_5OH)_4][TFSA]_2$ is shown in Figure 7. These $[Mg(C_2H_5OH)_4][TFSA]_2$ units were interconnected to a 3D structure only by *D*–H···A interactions (see Table S7 and Figure S8 for details). It should be noted that the O···H distances of O6–H6o···O2 and O5–H5o···O1 were 2.07 Å and 2.01 Å, respectively, which is significantly shorter than the sum of van der Waals radii of oxygen and hydrogen atoms (2.72 Å [26]).

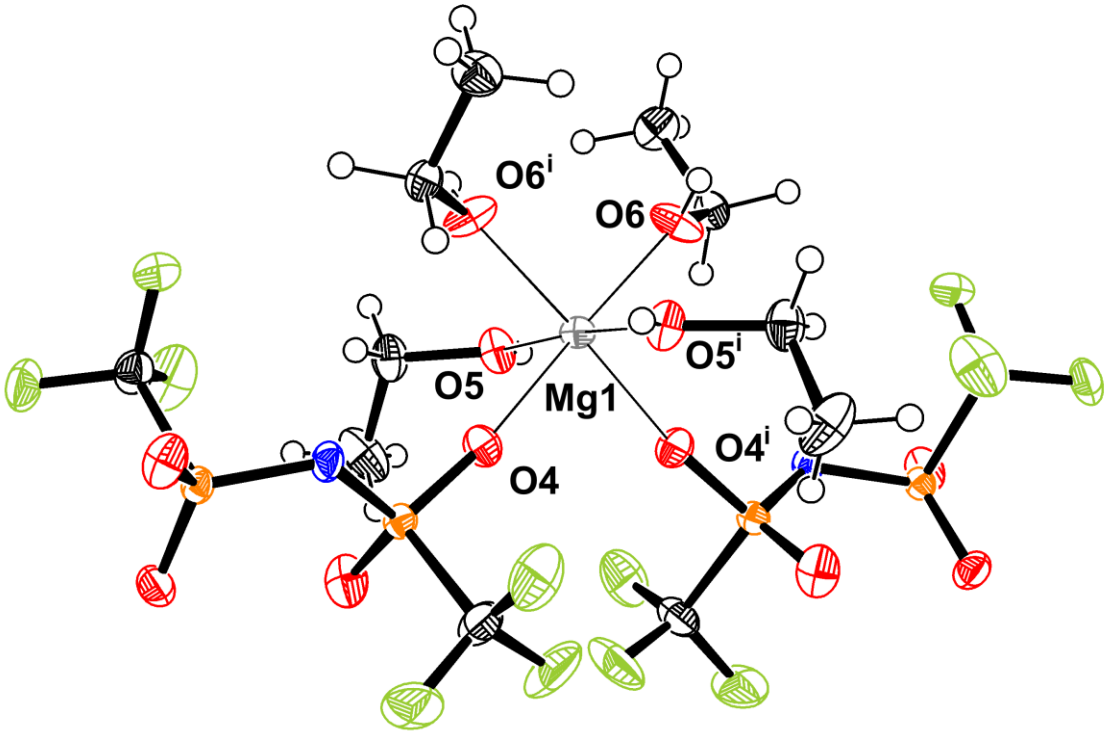

Figure 6. Coordination environment of Mg^{2+} in $[Mg(C_2H_5OH)_4][TFSA]_2$. Thermal ellipsoids are given at the 50% probability level (symmetry operations: (i) –*x*, *y*, ½–*z*).

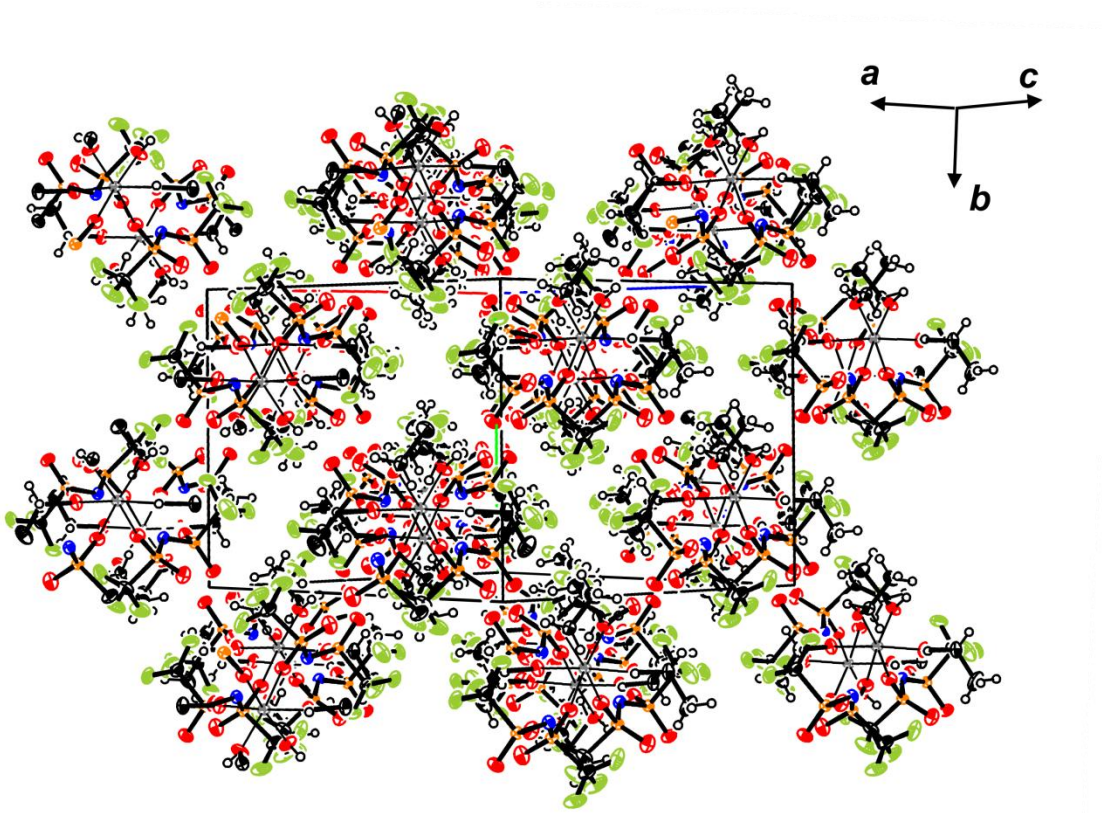

Figure 7. Packing diagram for $[Mg(C_2H_5OH)_4][TFSA]_2$. Thermal ellipsoids are given at the 30% probability level.

$[Mg(C_2H_5OH)_6][TFSA]_2$ and $[Mg(H_2O)_6][TFSA]_2(H_2O)_2$

Contrary to the experiment with chloroform containing a trace amount of ethanol, recrystallization from ethanol solution led to formation of the adduct form with six ethanol molecules bound to Mg^{2+}, $[Mg(C_2H_5OH)_6][TFSA]_2$. The structure of another salt containing eight water molecules, $[Mg(H_2O)_6][TFSA]_2(H_2O)_2$, has already been reported,[9, 17] and was repeatedly formed during longer exposure of the $Mg[TFSA]_2$ coordination compounds to air due to moisture uptake. $[Mg(H_2O)_6][TFSA]_2(H_2O)_2$ was found to be unstable in a dry stream of nitrogen at room temperature, and lost water molecules to become powdery. Diffraction data was recorded at 113 K and the cell parameters were slightly different to those determined at 295 K in a previous report (see Table 1).[9]

Figure 8 shows the molecular structures of $[Mg(C_2H_5OH)_6][TFSA]_2$ (disorder of ethanol molecules is omitted for clarity; for the disordered part see Figure S9) and $[Mg(H_2O)_6][TFSA]_2(H_2O)_2$. In both these compounds, Mg^{2+} was homoleptically coordinated to six ligands, giving rise to octahedral $Mg(C_2H_5OH)_6^{2+}$ and $Mg(H_2O)_6^{2+}$ units. The asymmetric unit of the salt with ethanol, $[Mg(C_2H_5OH)_6][TFSA]_2$, contained Mg^{2+}, three ethanol molecules, and one $TFSA^-$. All three crystallographically independent ethanol units were disordered. The asymmetric unit of $[Mg(H_2O)_6][TFSA]_2(H_2O)_2$ involved the octahedral $Mg(H_2O)_6^{2+}$ unit, two $TFSA^-$ anions, and two non-coordinating water molecules.

The first homoleptic $Mg(C_2H_5OH)_6^{2+}$ unit was determined by Valle and co-workers in the structure of $[Mg(C_2H_5OH)_6]Cl_2$.[27] The Mg···O distances determined in $[Mg(C_2H_5OH)_6][TFSA]_2$ ranged from 2.045(2) to 2.063(2) Å and were close to 2.069(3) Å in $[Mg(C_2H_5OH)_6]Cl_2$.[27] The O···Mg···O angles formed between two oxygen atoms from two ethanol molecules in *cis*-positions varied from 86.47(11)° for $O17^{i}$···Mg1···O14 to 93.53(11)°

for O17···Mg1···O14, whereas those in *trans*-positions were 180° with the symmetrical restriction.

The Mg···O distances in $[Mg(H_2O)_6][TFSA]_2(H_2O)_2$ ranged from 2.0410(10) Å (Mg1···O4) to 2.0642(10) Å (Mg1···O1), with the octahedron slightly distorted from the ideal shape. The O···Mg···O angles in *cis* positions varied from 86.98(4)° for O4···Mg1···O3 to 91.37(4)° for O4···Mg1···O6, whereas those in *trans* positions were between 178.33(4)° (O5···Mg1···O6) and 177.56(4)° (O3···Mg1···O1) (see Tables S8 and S9 for details of other bond lengths and angles in $[Mg(C_2H_5OH)_6][TFSA]_2$ and $[Mg(H_2O)_6][TFSA]_2(H_2O)_2$). $TFSA^-$ anions in both structures adopt *trans* conformations, which is common for weakly-bonded anions[9] (see Table 3 for details). The packing diagrams for both compounds are shown in Figure 9 (see Tables S10 and S11 for the *D*–H···A interactions in $[Mg(C_2H_5OH)_6][TFSA]_2$ and $[Mg(H_2O)_6][TFSA]_2(H_2O)_2$, respectively). It should be noted that no *D*–H···A interactions were below the van der Waals radii observed with F atoms.

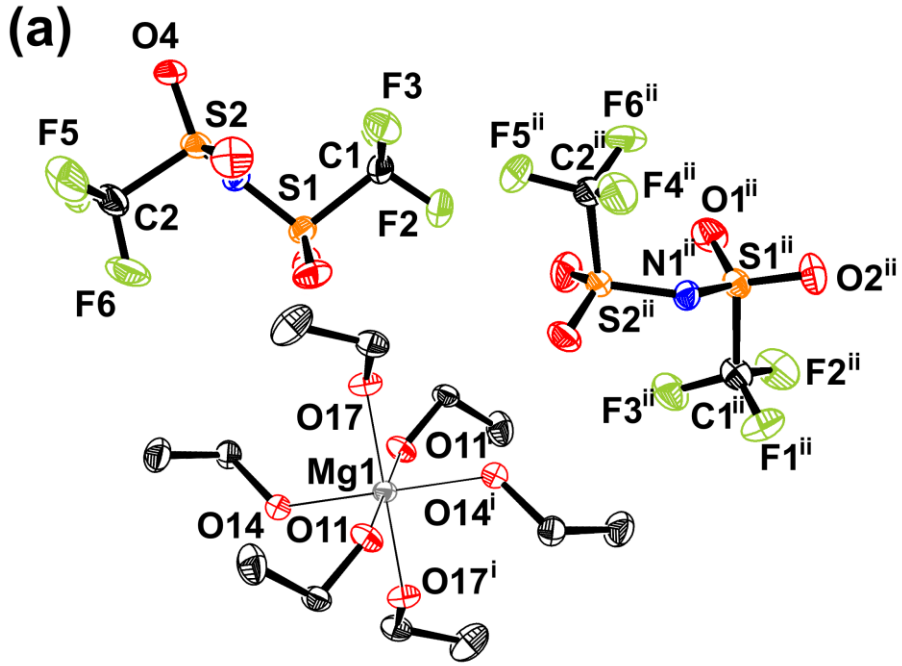

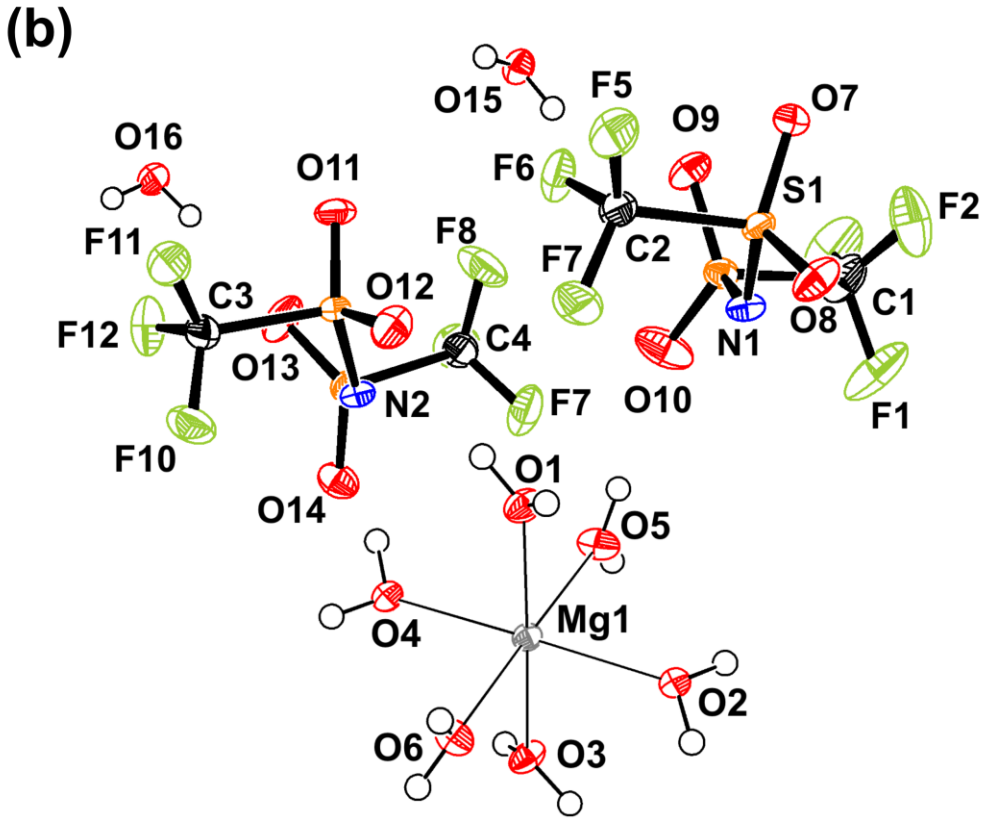

Figure 8. Molecular structures of (a) $[Mg(C_2H_5OH)_6][TFSA]_2$ (disordered part is omitted for clarity) and (b) $[Mg(H_2O)_6][TFSA]_2(H_2O)_2$. Thermal ellipsoids are given at (a) the 30% and (b) 50% probability levels (symmetry codes for (a): (i) $-x, -y, -z$, (ii) $-x+½, y+½, -z+½$).

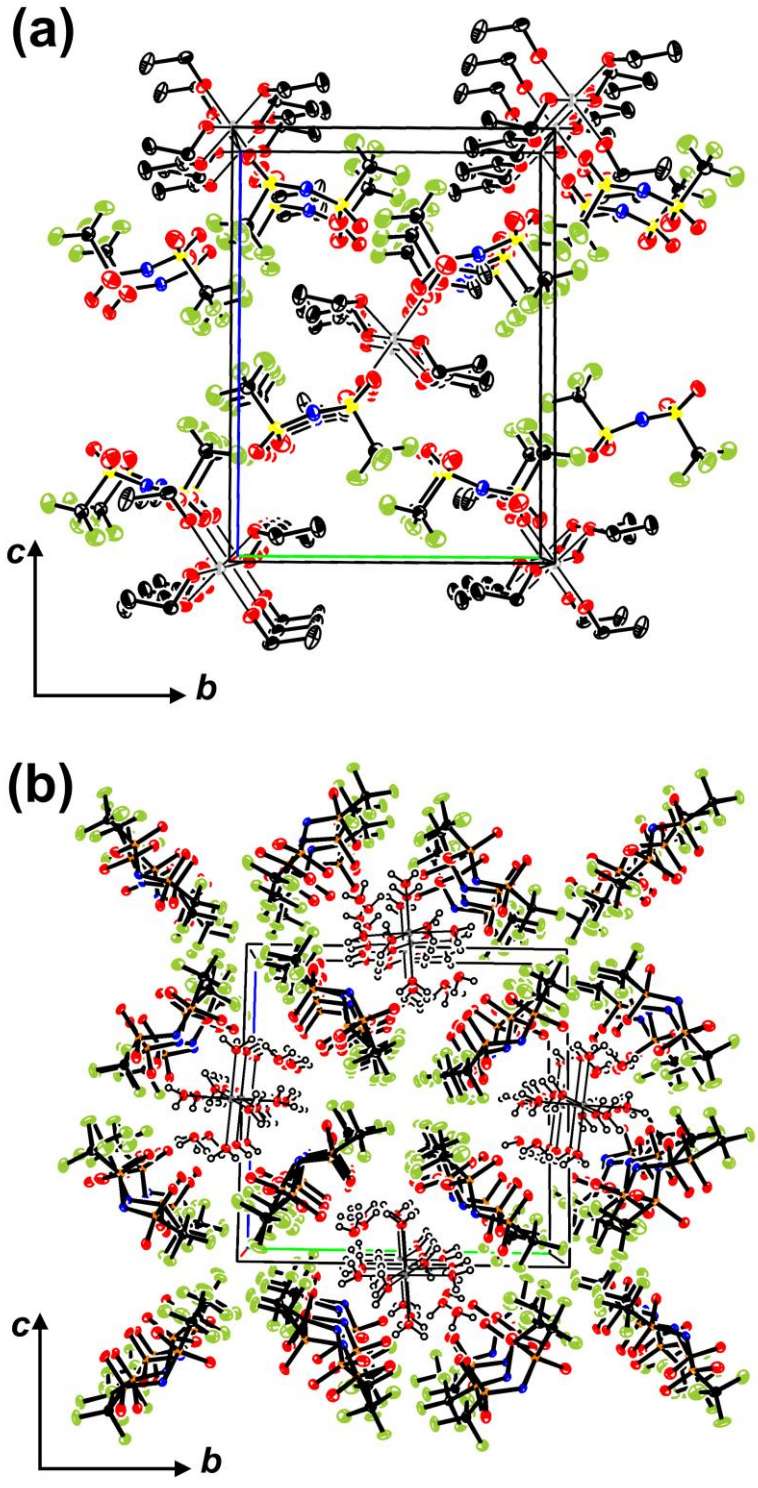

Figure 9. Packing diagrams for (a) $[Mg(C_2H_5OH)_6][TFSA]_2$ and (b) $[Mg(H_2O)_6][TFSA]_2(H_2O)_2$. Thermal ellipsoids are given at the 30% probability level. Hydrogen atoms and a disordered part of $[Mg(C_2H_5OH)_6][TFSA]_2$ are omitted for clarity.

Stepwise structural changes of Mg^{2+} and conformational changes of $TFSA^-$ during ligand attachment

There seem to be three main aspects determining the structural modalities of $Mg[TFSA]_2$ coordination compounds based on previous studies and the present work. Firstly, all structures contain hydrophobic domains made from CF_3 groups of the $TFSA^-$ anions and ligand alkyl groups. Secondly, Mg^{2+} readily coordinates to any σ-donor ligand (containing O or N)[2n] and an increase in ligands doubtless leads to the exclusion of $TFSA^-$ anions from the coordination sphere of Mg^{2+}. Finally, the solvation of $Mg[TFSA]_2$ appears to occur in a stepwise manner, where each step involves coordination of two ligands to the Mg^{2+} core (see below for details). To our knowledge, there is no example of an odd number of ligands connected to an Mg^{2+} core in a crystal lattice.

The coordination structures resemble each other in salts containing the same number of ligand molecules if the ligands have comparable sizes. For instance, $[Mg(C_2H_5OOCCH_3)_2][TFSA]_2$ and $[Mg(H_2O)_2][TFSA]_2$ have similar 1D chains (…–$(L)_2$–Mg^{2+}–$(L)_2$–…). Although there is currently no experimental example of Mg^{2+} with four water molecules in a TFSA salt, a similar example was reported for $[Mg(H_2O)_4][MSA]_2$,[25] in which the MSA^- anion adopts a *trans* conformation, similarly to $TFSA^-$ in $[Mg(C_2H_5OH)_4][TFSA]_2$. Analogously, Mg^{2+} has a homoleptic coordination sphere in $[Mg(C_2H_5OH)_6][TFSA]_2$, $[Mg(CH_3CN)_6][TFSA]_2$,[2n] and $[Mg(H_2O)_6][TFSA]_2(H_2O)_2$.

Although there is no complete set of $[Mg(L)_n][TFSA]_2$ (n = 0, 2, 4, and 6) with the same ligand, the stepwise structural changes in Mg^{2+} coordination with the formation of $[Mg(L)_n][TFSA]_2$ are proposed in Figure 10 by considering the known structures (one of the two disordered parts with the *cis* conformer in $Mg[TFSA]_2$ is omitted for clarity).

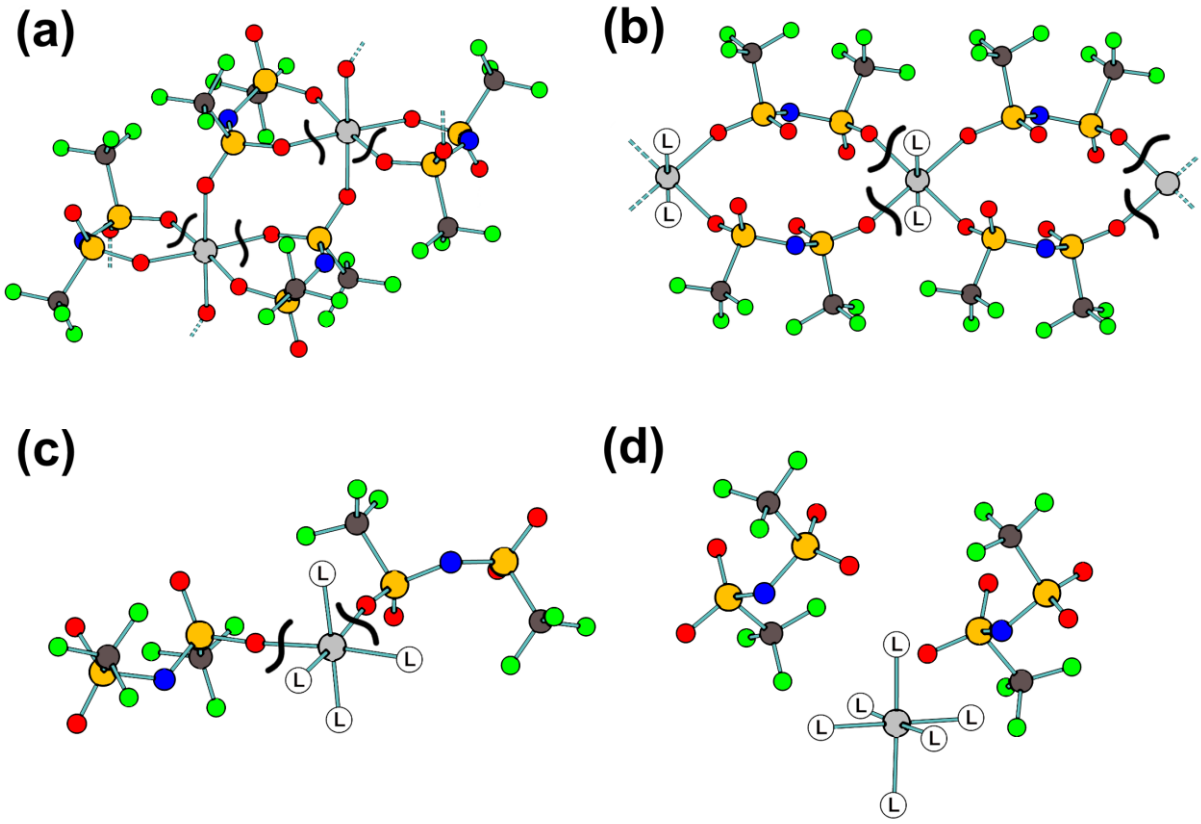

Figure 10. A proposed scheme for the stepwise solvation of Mg^{2+} in $Mg[TFSA]_2$ coordination compounds. Crossed lines are those most likely to break upon addition of ligand molecules to the Mg^{2+} core: (a) initial stage, pure $Mg[TFSA]_2$ structure; (b) second stage, di-substituted compound structure, $[Mg(L)_2][TFSA]_2$; (c) third stage, tetra-substituted compound structure, $[Mg(L)_4][TFSA]_2$; and (d) final stage, homoleptic $Mg(L)_6^{2+}$ unit surrounded by $TFSA^-$ anions.

The $TFSA^-$ anions in $Mg[TFSA]_2$ are deformed by chelating to a small Mg^{2+} core via two different SO_2 groups. At first, the ligand approaches the Mg center to split the chains in the structure of $Mg[TFSA]_2$. One chelating Mg···O contact breaks first, creating space for a ligand, followed by a flipping of the ligand arrangement around Mg^{2+} (Figure 10 (a)). The resulting chain in $[Mg(L)_2][TFSA]_2$ has two ligands in *trans* positions and four bridging $TFSA^-$ anions in the coordination sphere of Mg^{2+}. During further breaking of this chain

(Figure 10 (b)), two more $Mg^{2+}\cdots TFSA^{-}$ contacts are substituted by two ligands, resulting in discrete $[Mg(L)_4][TFSA]_2$ units (Figure 10 (c)) that are interconnected only by C−H···O interactions. As the final step, the two residual contacts between the Mg^{2+} core and the anions break and two more ligands enter to give the final homoleptic octahedral complex, $Mg(L)_6^{2+}$ (see Figure 10 (d)). The only step of solvation in which $TFSA^{-}$ anions have a *cis* conformation is the chain containing two ligands bound to different Mg^{2+} cores, $[Mg(L)_2][TFSA]_2$ (without taking into consideration the disordered part in pure $Mg[TFSA]_2$). The structural change suggested was consistent for all the crystal structures discussed in previous and the present work.[2n, 14, 17] This suggested that the $TFSA^{-}$ anion conformation in a coordination environment with monodentate ligands is determined by the number of ligands bound to the Mg^{2+} core. However, the structure might be different in the case of bulky ligands due to steric reasons. For instance, a ligand containing oxygen or nitrogen and a large apolar organic frame, such as polycyclic hydrocarbons, could displace $TFSA^{-}$ anions from the coordination sphere of Mg^{2+}. To our knowledge, there is no data on coordination compounds of $Mg[TFSA]_2$ with such bulky ligands.

Vibrational spectroscopy

Vibrational modes of $TFSA^{-}$ were first analyzed by Rey *et al.* using *ab initio* calculations for the *trans* conformer.[2a] Later, normal coordinate analysis was also carried out for the *cis* conformer.[20a] Raman spectroscopy can be used to reveal the coordination state of $TFSA^{-}$ anions at a metal core in the solid and liquid states, including ionic liquids.[2n, 20b, 28] For instance, the most intensive band in the spectrum of $M[TFSA]_n$ (M = metal cation) relates to the combination of $\delta_s(CF_3)+\upsilon_s(SNS)$, and should appear at around 750 cm^{-1}.[2h, 2i, 20b, 28-29] The shift of this band to a higher frequency indicates a stronger interaction of $TFSA^{-}$ with the

metal core and *vice versa*.[20b, 30] In inorganic salts, $TFSA^-$ is usually connected to the metal core via M···O contact; the only example of the salt having M···N interactions in the solid state is in Cs[TFSA].[13, 31] The conformation of $TFSA^-$ was also derived from Raman spectroscopy. According to literature sources, $\omega(SO_2)$ (ω = wagging) band is used for the identification of $TFSA^-$ conformation,[2h, 20a, 29-30, 32] and is expected to appear at around 398 and 407 cm^{-1} for *trans* and *cis* conformers, respectively, according to work on $[C_2C_1im][TFSA]$ (C_2C_1im = 1-ethyl-3-methylimidazolium) ionic liquid.[20a] Below, the Raman spectra of $Mg[TFSA]_2$ single salt and its coordination compounds are described. The $TFSA^-$ bands were of most interest, describing the bond strength with the Mg^{2+} core and anion conformations. Discussion of ligand vibrational bands is omitted due to low interest. The Raman spectra of $Mg[TFSA]_2$, $[Mg(C_2H_5OH)_4][TFSA]_2$, $[Mg(C_2H_5OH)_6][TFSA]_2$, and $[Mg(H_2O)_6][TFSA]_2(H_2O)_2$ are shown in Figure 11, and band assignments are listed in Table 4. The Raman spectrum of ethanol, used to identify bands assigned to the ethanol ligand, is shown in Figure S10. All attempts to record the Raman spectra of $[Mg(H_2O)_2][TFSA]_2$ and $[Mg(C_2H_5OOCCH_3)_2][TFSA]_2$ failed due to high fluorescence. In our recent work,[2n] we used the Raman spectrum of pure $Mg[TFSA]_2$ powder to identify bands in the spectrum of $Mg[TFSA]_2$–acetonitrile electrolytes. In the present work, we report the Raman spectrum recorded for a $Mg[TFSA]_2$ single crystal grown by sublimation.

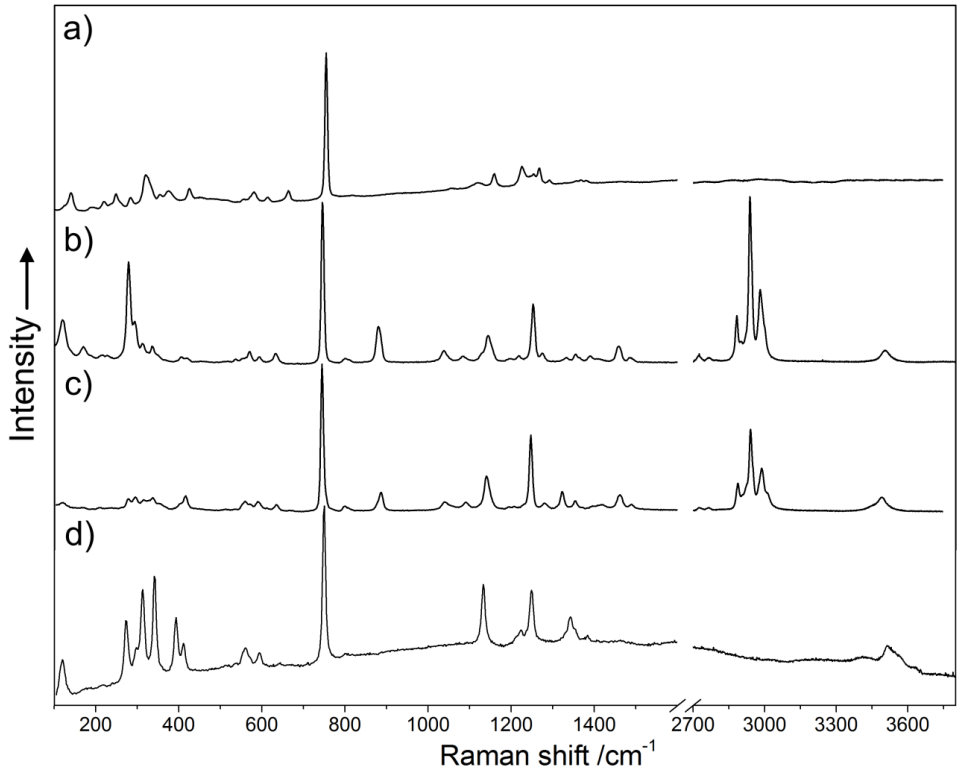

Figure 11. Raman spectra of (a) $Mg[TFSA]_2$, (b) $[Mg(C_2H_5OH)_4][TFSA]_2$, (c) $[Mg(C_2H_5OH)_6][TFSA]_2$, and (d) $[Mg(H_2O)_6][TFSA]_2(H_2O)_2$.

Although no bands were observed above 1400 cm^{-1} for pure $Mg[TFSA]_2$, the bands assigned to O−H stretching appeared at around 3500 cm^{-1}, even after brief exposure to air, indicating the presence of water molecules in the structure (Figure S11). The spectrum was rather different from those of $Mg[TFSA]_2$ and $[Mg(H_2O)_6][TFSA]_2(H_2O)_2$ (discussed later, see Figure 11 and Table 4).

The most intensive band in the spectrum of $Mg[TFSA]_2$ was observed at 754 cm^{-1}, which correlated with the spectrum recorded for powder in our previous work[2n] and matched the frequency from Giffin *et al.*[20c] The $\omega(SO_2)$ bands corresponding to both *cis* and *trans*

conformers of $TFSA^-$ in the disordered states (Figure 1) were observed at 374 and 424 cm^{-1}, respectively. This work suggests that coordination environment results in a red shift of the $\omega(SO_2)$ band for the *trans* conformer, and a blue shift for the *cis* conformer. This was consistent with the spectra of other compounds obtained in this work; for instance, $TFSA^-$ anions in $[Mg(C_2H_5OH)_6][TFSA]_2$ have *trans* conformation and corresponding band appeared at 416 cm^{-1} (see Table 4 for other $\omega(SO_2)$ band positions).

$TFSA^-$ anions in $[Mg(C_2H_5OH)_4][TFSA]_2$ adopted *trans* conformation and two $\omega(SO_2)$ bands were observed at 418 and 405 cm^{-1}. The band at 418 cm^{-1} was assigned to SO_2 groups bound to the Mg^{2+} core, while the band at 405 cm^{-1} was assigned to "free" SO_2 groups. The strongest bands from the $TFSA^-$ anions, $\delta(CF_3)+\upsilon_s(SNS)$, were observed at 745 and 744 cm^{-1} in the spectra of $[Mg(C_2H_5OH)_4][TFSA]_2$ and $[Mg(C_2H_5OH)_6][TFSA]_2$, respectively. The shift of this band from 754 cm^{-1} in pure $Mg[TFSA]_2$ indicated that interactions between the anion and Mg^{2+} core in the ethanol coordination compounds were weaker than in pure $Mg[TFSA]_2$. Surprisingly, this band appeared in a similar position in these spectra, despite the absence of direct $Mg^{2+}\cdots TFSA^-$ interaction in $[Mg(C_2H_5OH)_6][TFSA]_2$. This may be due to the contribution of C−H···O interactions between the ethanol ethyl group and O atoms in the anion. The $\nu(Mg\cdots O)$ bands appeared at 278 cm^{-1} in the spectrum of $[Mg(C_2H_5OH)_4][TFSA]_2$. In a homoleptic octahedral complex, two bands, A_{1g} and E_g, should be active in the Raman spectrum.[2n] The lowering of symmetry in $[Mg(C_2H_5OH)_6][TFSA]_2$, leading to the presence of three crystallographically independent ethanol molecules, should result in more Raman-active bands. The only $\nu(Mg\cdots O)$ band at 278 cm^{-1} with low intensity was observed in the spectrum of $[Mg(C_2H_5OH)_6][TFSA]_2$; presumably, other $\nu(Mg\cdots O)$ bands were of too low intensity to be detected.

Table 4. Selected Raman frequencies, intensities, and assignments for $Mg[TFSA]_2$, $[Mg(C_2H_5OH)_4][TFSA]_2$, $[Mg(C_2H_5OH)_6][TFSA]_2$, and $[Mg(H_2O)_6][TFSA]_2(H_2O)_2$. [a]

Raman frequency / cm^{-1}				Assignment[1]
$Mg[TFSA]_2$	$[Mg(C_2H_5OH)_4][TFSA]_2$	$[Mg(C_2H_5OH)_6][TFSA]_2$	$[Mg(H_2O)_6][TFSA]_2(H_2O)_2$	
140(12)	119(26)	119(4)	119(22)	
191(1)	169(9)	169(1)		deformation modes
219(4)	215(4)	209(1)		
249(9)	227(4)			
282(6)	278(63)	278(7)	272(41)	ν(Mg···O)
319(20)	294(25)	295(8)	298(23)	δ(FCS)
	311(11)	315(6)	313(61)	$\rho(SO_2)$
355(6)	335(10)	336(8)	341(62)	$\tau(SO_2)$
			393(35)	ν(Mg···O)
374(3)	405(3)			$\omega(SO_2)$
424(7)	418(2)	416(9)	410(17)	
	537(2)			$\delta_a(CF_3)$
581(6)	569(6)	559(5)	559(12)	
		570(3)		-
	593(3)	589(5)	593(9)	$\delta_a(SO_2)$
613(3)		612(1)		-
663(8)	633(5)	634(3)		δ(SNS)
754(100)	745(100)	744(100)	750(100)	$\delta(CF_3)+\upsilon_s$(SNS)
816(1)	800(2)	799(2)		$\upsilon_s(CF_3)$
	880(22)	887(11)		*
	1037(7)	1039(5)		*
	1083(3)	1090(5)		*
1120(3)	1143(16)	1139(23)	1133(39)	$\upsilon_s(SO_2)$
1159(9)				
	1197(2)	1195(1)		$\upsilon_s(CF_3)$
1225(13)	1218(4)	1205(2)	1223(9)	
1252(8)	1252(36)	1246(51)	1249(34)	$\upsilon_s(SO_2)$
1266(12)	1275(5)	1280(4)		$\delta_s(CF_3)$
1292(3)				
	1333(3)	1322(12)	1343(16)	*
1357(3)	1354(5)	1354(6)	1384(5)	$\upsilon_a(CF_3)$
1367(4)				$\upsilon_a(SO_2)$
1380(3)	1389(4)	1420(3)		
	1459(10)	1462(10)		*
	1486(3)	1489(3)		*

[a] Frequencies assigned to the anion are given in cm^{-1}. Intensities are scaled relative to the intensity of the $\delta(CF_3)+\upsilon_s$(SNS) mode, which is assigned a value of 100. [1] Symbols denote the following: υ_a, asymmetric stretching; υ_s, symmetric stretching; δ_s, scissoring; ρ, rocking; ω, wagging; and τ, twisting. Assignments are based on previous reports.[2a, 30] The symbol * denotes bands assigned to the ligands.

In the Raman spectrum of $[Mg(H_2O)_6][TFSA]_2(H_2O)_2$ (Figure 11 (d)), the $\omega(SO_2)$ band of $TFSA^-$ appeared at 410 cm^{-1}, which was close to the value reported for $[C_2C_1im][TFSA]$ ionic liquid (407 cm^{-1}).[20a] The frequency of the $\delta(CF_3)+\upsilon_s(SNS)$ band of $TFSA^-$ (750 cm^{-1}) was higher than that observed for the ethanol adduct, but still lower than that of pure $Mg[TFSA]_2$. This may be explained by the presence of strong O_{Et}–H···O_{an} interactions (O_{Et} = O atom in ethanol molecule and O_{an} = O atom in $TFSA^-$; e.g. H···O_{an} distances are below 2 Å for O17–H17···O1 and O11–H11···O2; see Table S10), which causes a red shift and mimics the band shift in compounds with $TFSA^-$ coordinated to a metal core. According to the work of Pye and Rudolph,[33] the symmetric ν(Mg···O) (A_{1g}) of $Mg(H_2O)_6^{2+}$ units appears at 354–356 cm^{-1} in water solutions of $MgSO_4$ and $Mg(ClO_4)_2$ and could appear at lower frequencies in crystals due to the lattice influence. Since the crystal structure indicated that $TFSA^-$ adopted *trans* conformation in $[Mg(H_2O)_6][TFSA]_2(H_2O)_2$, the band at 393 cm^{-1} was tentatively assigned to the E_g (ν(Mg···O)) mode of the $Mg(H_2O)_6^{2+}$ octahedral complex. The $\omega(SO_2)$ band appeared at 410 cm^{-1}, close to the same band of *trans*-$TFSA^-$ in the spectra of $Mg[TFSA]_2$ and its ethanol adduct.

Conclusions

In the present work, the coordination environments of Mg^{2+} in $Mg[TFSA]_2$ and its adducts, $[Mg(C_2H_5OOCCH_3)_2][TFSA]_2$, $[Mg(H_2O)_2][TFSA]_2$, $[Mg(C_2H_5OH)_4][TFSA]_2$, $[Mg(C_2H_5OH)_6][TFSA]_2$, and $[Mg(H_2O)_6][TFSA]_2(H_2O)_2$, were discussed based on their single-crystal X-ray diffraction data and Raman spectroscopy. $Mg[TFSA]_2$ is the first example of a structure containing disordered *cis* and *trans* $TFSA^-$ conformers. In all the compounds prepared, Mg^{2+} had octahedral surroundings consisting of O atoms either from ligands or $TFSA^-$ anions. The new and previously known salts provide a stepwise change in

coordination environment, from $Mg[TFSA]_2$ to the homoleptic $[MgL_6][TFSA]_2$ via the …−$(L)_2$−Mg^{2+}−$(L)_2$−… double-bridging 1D chain and the isolated [$TFSA^-$]−[$Mg^{2+}(L)_4$]−[$TFSA^-$] unit. The scheme for stepwise ligand accession to Mg^{2+} in $Mg[TFSA]_2$ discovered herein indicates that $TFSA^-$ anion conformation is determined by the number of ligands in the coordination sphere of Mg^{2+}, which is restricted to even numbers only.

Experimental Section

Reagents and chemicals

Volatile materials were handled in a vacuum line constructed using stainless steel, Pyrex glass, and tetrafluoroethylene−perfluoroalkylvinylether copolymer. Nonvolatile materials were handled under a dry argon atmosphere in a glovebox or a dry air atmosphere in a dry chamber. $Mg[TFSA]_2$, (Kishida Chemicals, purity 99.9 %) was dried under vacuum at room temperature for 6 h and then for 24 h at 200 °C. Karl-Fischer titration indicated the water content of 200 ppm. Ethanol (Wako Chemicals, super dehydrated, purity 99.8%, water content <10 ppm), chloroform (Wako Chemicals, super dehydrated, purity 99% (stabilized by ethanol, 0.3–1%), water content <10 ppm), ethyl acetate (Wako Chemicals, super dehydrated, purity 99.5%, water content <10 ppm), and nitromethane (Aldrich Co., purity ≥98.5%, water content ≤100 ppm) were used as received.

Caution: Fluorine containing compounds could be hazardous. Special attention should be paid during experiments.

Crystal growth

Crystals of $Mg[TFSA]_2$ were grown by sublimation. A portion of $Mg[TFSA]_2$ powder (approximately 40 mg) was placed at the bottom of a Pyrex glass ampoule, which was then evacuated for 5 min (residual pressure ~1 Pa) and sealed. Heating at 300 °C for 20 h under a

static vacuum resulted in the sublimate growth as a needle crystal. When $Mg[TFSA]_2$ was not dry enough, two zones formed during sublimation; a low temperature zone covered with tiny $[Mg(H_2O)_2][TFSA]_2$ plates and a higher temperature zone containing $Mg[TFSA]_2$ needles. Crystals of $[Mg(C_2H_5OOCCH_3)_2][TFSA]_2$ were grown by slowly cooling the saturated ethyl acetate solution of $Mg[TFSA]_2$ with the residual $Mg[TFSA]_2$ from 60 °C to room temperature. Crystals of $[Mg(H_2O)_2][TFSA]_2$ were grown in a poly(tetrafluoroethylene) pressure resistant container by slowly cooling the dichloromethane solution of $Mg[TFSA]_2$. Water, present as an impurity in dichloromethane, became coordinated to Mg^{2+} and incorporated into the crystal lattice. Another approach leading to the formation of $[Mg(H_2O)_2][TFSA]_2$ crystals was the recrystallization of $Mg[TFSA]_2$ from nitromethane without pre-drying. $Mg[TFSA]_2$ (approx. 100 mg) was dissolved in 3 mL of hot nitromethane (approximately 50 °C). The resulting solution was cooled, reduced in volume by solvent removal under dynamic vacuum, and stored at 10 °C; crystals appeared within two days. $[Mg(C_2H_5OH)_4][TFSA]_2$ crystals were grown from the chloroform solution of $Mg[TFSA]_2$ during attempted $Mg[TFSA]_2$ crystal growth, because the chloroform contained ethanol as a stabilizer. $Mg[TFSA]_2$ (approx. 50 mg) was dissolved in 1 mL of hot chloroform (50°C) and the resulting solution was stored at 10 °C, affording colorless crystals in five days. $[Mg(C_2H_5OH)_6][TFSA]_2$ crystals were grown in conditions analogous to those of $[Mg(C_2H_5OH)_4][TFSA]_2$. $Mg[TFSA]_2$ (approx. 50 mg) was dissolved in 1 mL of hot chloroform. Ethanol (0.08 mL) was added with an Eppendorf syringe, and the resulting solution was placed in a fridge (~10 °C). Colorless crystals appeared within three days. $[Mg(H_2O)_6][TFSA]_2(H_2O)_2$ crystals appeared in various solvents at the final stage of saturation with moisture from the air. The best quality crystals were obtained from a chloroform/water solution. $Mg[TFSA]_2$ (85 mg) was dissolved in 4.5 mL of hot chloroform, and 0.1 mL of distilled water was added using a syringe. Colorless

crystals of $[Mg(H_2O)_6][TFSA]_2(H_2O)_2$ appeared within one week, keeping the solution at 10 °C.

Single crystal X-ray crystallography

Crystals of $Mg[TFSA]_2$, $[Mg(C_2H_5OH)_4][TFSA]_2$, $[Mg(C_2H_5OH)_6][TFSA]_2$, $[Mg(H_2O)_2][TFSA]_2$, and $[Mg(H_2O)_6][TFSA]_2(H_2O)_2$ suitable for X-ray diffraction were selected in the dry chamber and glued to a quartz pin using perfluoroether oil. In the case of $[Mg(C_2H_5OOCCH_3)_2][TFSA]_2$, the crystal was fixed in a quartz capillary in a glovebox. The pin was transferred to the goniometer head (Rigaku R-axis Rapid II, controlled by the program RAPID AUTO 2.40,[34] equipped with image-plate area detector and graphite-monochromated Mo-Kα tube (0.71073 Å)) and placed in a stream of cold nitrogen. The X-ray output was 40 mA at 50 kV.

Integration, scaling and absorption corrections were performed using RAPID AUTO 2.40 software.[34] The structure was solved using SIR-2008,[35] SIR-2014,[36] and refined by SHELXL-97[37] in WinGX software.[38] Ortep 3[39] was used to visualize the crystal structures.

Raman spectroscopy

All spectra were recorded using a Nanofinder 30 (Tokyo Instruments) microfocus Raman spectrometer with a 632 nm He-Ne laser. The Raman spectrum of $Mg[TFSA]_2$ crystals was recorded through the glass ampoule after sublimation was complete. The adducts were sealed in 1 mm glass capillaries under a dry atmosphere to avoid the presence of water, and Raman spectra were recorded through the glass walls. The band of polycrystalline Si (520.6 cm^{-1}) was used to calibrate the spectrometer before each measurement.

DSC

Thermal analysis for the $Mg[TFSA]_2$ sample was performed by using a differential scanning calorimeter (DSC-60, Shimadzu). The samples were sealed in Al cells under a dry air atmosphere. The scan rate used for the measurements was 10 K min^{-1}, and the machine was flushed with Ar for 10 min prior to every measurement.

Electronic Supplementary Information

Electronic Supplementary Information available: Selected bond lengths (Å) and angles (˚) in the compounds prepared and details on *D*-H···A interactions (Tables S1-S11), possible conformations of $TFSA^-$ anion (Figure S1), packing diagram of $Mg[TFSA]_2$ containing *cis* conformers of $TFSA^-$ (Figure S2), XRD powder patterns of $Mg[TFSA]_2$ (Figure S3), DSC curves recorded on $Mg[TFSA]_2$ powder (Figure S4), the asymmetric unit of $[Mg(C_2H_5OOCCH_3)_2][TFSA]_2$ (Figure S5), the disordered ethyl acetate ligands in $[Mg(C_2H_5OOCCH_3)_2][TFSA]_2$ (Figure S6), representation of *D*–H···A interactions in $[Mg(H_2O)_2][TFSA]_2$ (Figure S7), the *D*–H···A interactions of $TFSA^-$ in $[Mg(C_2H_5OH)_4][TFSA]_2$ (Figure S8), the homoleptic $[Mg(C_2H_5OH)_6]^{2+}$ unit in the structure of $[Mg(C_2H_5OH)_6][TFSA]_2$ (Figure S9), Raman spectrum of ethanol (Figure S10), the Raman spectrum of $Mg[TFSA]_2$ after exposure to the air (Figure S11).

ACKNOWLEDGEMENTS

This work was financially supported by the Grant-in-Aid for Scientific Research of Japan Society for the Promotion of Science, #26·04763.

REFERENCES

[1] J. Foropoulos, D. D. DesMarteau, *J. Am. Chem. Soc.* **1982**, *104*, 4260-4261.

[2] a) I. Rey, P. Johansson, J. Lindgren, J. C. Lassègues, J. Grondin, L. Servant, *J. Phys. Chem. A* **1998**, *102*, 3249-3258; b) W. Gorecki, M. Jeannin, E. Belorizky, C. Roux, M. Armand, *J. Phys.: Condens. Matter* **1995**, *7*, 6823; c) A. Vallée, S. Besner, J. Prud'Homme, *Electrochim. Acta* **1992**, *37*, 1579-1583; d) J. L. Paul, C. Jegat, J. C. Lassègues, *Electrochim. Acta* **1992**, *37*, 1623-1625; e) M. Hernandez, L. Servant, J. Grondin, J. C. Lassègues, *Ionics* **1995**, *1*, 454-468; f) S. Duluard, J. Grondin, J.-L. Bruneel, I. Pianet, A. Grélard, G. Campet, M.-H. Delville, J.-C. Lassègues, *J. Raman Spectrosc.* **2008**, *39*, 627-632; g) J. C. Lassègues, J. Grondin, R. Holomb, P. Johansson, *J. Raman Spectrosc.* **2007**, *38*, 551-558; h) J.-C. Lassègues, J. Grondin, C. Aupetit, P. Johansson, *J. Phys. Chem. A* **2009**, *113*, 305-314; i) J.-C. Lassegues, J. Grondin, D. Talaga, *Phys. Chem. Chem. Phys.* **2006**, *8*, 5629-5632; j) S.-Y. Ha, Y.-W. Lee, S. W. Woo, B. Koo, J.-S. Kim, J. Cho, K. T. Lee, N.-S. Choi, *ACS Appl. Mater. Interfaces* **2014**, *6*, 4063-4073; k) T. T. Tran, W. M. Lamanna, M. N. Obrovac, *J. Electrochem. Soc.* **2012**, *159*, A2005-A2009; l) Y. Orikasa, T. Masese, Y. Koyama, T. Mori, M. Hattori, K. Yamamoto, T. Okado, Z.-D. Huang, T. Minato, C. Tassel, J. Kim, Y. Kobayashi, T. Abe, H. Kageyama, Y. Uchimoto, *Sci. Rep.* **2014**, *4*, 5622; m) T. S. Arthur, N. Singh, M. Matsui, *Electrochem. Commun.* **2012**, *16*, 103-106; n) G. Veryasov, K. Matsumoto, R. Hagiwara, *Dalton Trans.* **2016**, *45*, 2810-2813.

[3] a) S. Seki, Y. Ohno, Y. Kobayashi, H. Miyashiro, A. Usami, Y. Mita, H. Tokuda, M. Watanabe, K. Hayamizu, S. Tsuzuki, M. Hattori, N. Terada, *J. Electrochem. Soc.* **2007**, *154*, A173-A177; b) S. Seki, Y. Kobayashi, H. Miyashiro, Y. Ohno, A. Usami, Y. Mita, N. Kihira, M. Watanabe, N. Terada, *J. Phys. Chem. B* **2006**, *110*, 10228-10230; c) S. Seki, Y. Kobayashi, H. Miyashiro, Y. Ohno, Y. Mita, A. Usami, N. Terada, M. Watanabe, *Electrochem. Solid-State Lett.* **2005**, *8*, A577-A578; d) D. B. Williams, M. E. Stoll, B. L. Scott, D. A. Costa, J. W. J. Oldham, *Chem. Commun. (Cambridge, U. K.)* **2005**, 1438-1440; e) J. M. Tarascon, M. Armand, *Nature* **2001**, *414*, 359-367.

[4] a) J. R. Atkins, C. R. Sides, S. E. Creager, J. L. Harris, W. T. Pennington, B. H. Thomas, D. D. DesMarteau, *J. New Mat. Electr. Sys.* **2003**, *6*, 9-15; b) J. L. Nowinski, P. Lightfoot, P. G. Bruce, *J. Mater. Chem.* **1994**, *4*, 1579-1580.

[5] H. Kobayashi, J. Nie, T. Sonoda, *Chem. Lett.* **1995**, *1995*, 307-308.

[6] M. J. Earle, U. Hakala, B. J. McAuley, M. Nieuwenhuyzen, A. Ramani, K. R. Seddon, *Chem. Commun. (Cambridge, U. K.)* **2004**, 1368-1369.

[7] a) D. Aurbach, Z. Lu, A. Schechter, Y. Gofer, H. Gizbar, R. Turgeman, Y. Cohen, M. Moshkovich, E. Levi, *Nature* **2000**, *407*, 724-727; b) H. D. Yoo, I. Shterenberg, Y. Gofer, G. Gershinsky, N. Pour, D. Aurbach, *Energy Environ. Sci.* **2013**, *6*, 2265-2279; c) M. Matsui, *J. Power Sources* **2011**, *196*, 7048-7055; d) Y. Kumar, S. A. Hashmi, G. P. Pandey, *Electrochim. Acta* **2011**, *56*, 3864-3873; e) E. Levi, Y. Gofer, D. Aurbach, *Chem. Mater.* **2010**, *22*, 860-868; f) F.-f. Wang, Y.-s. Guo, J. Yang, Y. Nuli, S.-i. Hirano, *Chem. Commun. (Cambridge, U. K.)* **2012**, *48*, 10763-10765; g) J. Muldoon, C. B. Bucur, A. G. Oliver, T. Sugimoto, M. Matsui, H. S. Kim, G. D. Allred, J. Zajicek, Y. Kotani, *Energy Environ. Sci.* **2012**, *5*, 5941-5950; h) R. Mohtadi, M. Matsui, T. S. Arthur, S.-J. Hwang, *Angew. Chem. Int. Ed.* **2012**, *51*, 9780-9783; i) H. S. Kim, T. S. Arthur, G. D. Allred, J. Zajicek, J. G. Newman, A. E. Rodnyansky, A. G. Oliver, W. C. Boggess, J. Muldoon, *Nat Commun* **2011**, *2*, 427.

[8] N. N. Rajput, X. Qu, N. Sa, A. K. Burrell, K. A. Persson, *J. Am. Chem. Soc.* **2015**, *137*, 3411-3420.

[9] L. Xue, D. D. DesMarteau, W. T. Pennington, *Solid State Sci.* **2005**, *7*, 311-318.

[10] L. Xue, D. D. DesMarteau, W. T. Pennington, *Angew. Chem. Int. Ed.* **1997**, *36*, 1331-1333.

[11] P. Johansson, S. P. Gejji, J. Tegenfeldt, J. Lindgren, *Electrochim. Acta* **1998**, *43*, 1375-1379.

[12] Z. Žák, A. Růžička, C. Michot, *Z. Kristallogr.* **1998**, *213*, 217.

[13] L. Xue, C. W. Padgett, D. D. DesMarteau, W. T. Pennington, *Solid State Sci.* **2002**, *4*, 1535-1545.
[14] L. Xue, C. W. Padgett, D. D. DesMarteau, W. T. Pennington, *Acta Crystallogr. Sect. C* **2004**, *60*, m200-m202.
[15] W. A. Henderson, D. M. Seo, Q. Zhou, P. D. Boyle, J.-H. Shin, H. C. De Long, P. C. Trulove, S. Passerini, *Advanced Energy Materials* **2012**, *2*, 1343-1350.
[16] J. D. Holbrey, W. M. Reichert, R. D. Rogers, *Dalton Trans.* **2004**, 2267-2271.
[17] A. Haas, C. Klare, P. Betz, J. Bruckmann, C. Krüger, Y. H. Tsay, F. Aubke, *Inorg. Chem.* **1996**, *35*, 1918-1925.
[18] W. A. Henderson, M. Herstedt, V. G. Young, S. Passerini, H. C. De Long, P. C. Trulove, *Inorg. Chem.* **2006**, *45*, 1412-1414.
[19] W. A. Henderson, V. G. Young, S. Passerini, P. C. Trulove, H. C. De Long, *Chem. Mater.* **2006**, *18*, 934-938.
[20] a) K. Fujii, T. Fujimori, T. Takamuku, R. Kanzaki, Y. Umebayashi, S.-i. Ishiguro, *J. Phys. Chem. B* **2006**, *110*, 8179-8183; b) T. Watkins, D. A. Buttry, *J. Phys. Chem. B* **2015**, *119*, 7003-7014; c) G. A. Giffin, A. Moretti, S. Jeong, S. Passerini, *J. Phys. Chem. C* **2014**, *118*, 9966-9973; d) T. Fujimori, K. Fujii, R. Kanzaki, K. Chiba, H. Yamamoto, Y. Umebayashi, S.-i. Ishiguro, *J. Mol. Liq.* **2007**, *131–132*, 216-224.
[21] M. J. Earle, B. J. Mcauley, A. Ramani, K. R. Seddon, J. M. Thomson, *World Patent, WO02072519* **2002**.
[22] K. Matsumoto, T. Matsui, T. Nohira, R. Hagiwara, *J. Fluorine Chem.* **2015**, *174*, 42-48.
[23] W. Grochala, M. K. Cyranski, M. Derzsi, T. Michalowski, P. J. Malinowski, Z. Mazej, D. Kurzydlowski, W. Kozminski, A. Budzianowski, P. J. Leszczynski, *Dalton Trans.* **2012**, *41*, 2034-2047.
[24] J. Utko, P. Sobota, T. Lis, K. Majewska, *J. Organomet. Chem.* **1989**, *359*, 295-300.
[25] D. Henschel, K. Linoh, K.-H. Nagel, A. Blaschette, P. G. Jones, *Z. Anorg. Allg. Chem.* **1996**, *622*, 1065-1075.
[26] A. Bondi, *J. Phys. Chem.* **1964**, *68*, 441-451.
[27] G. Valle, G. Baruzzi, G. Paganetto, G. Depaoli, R. Zannetti, A. Marigo, *Inorg. Chim. Acta* **1989**, *156*, 157-158.
[28] M. J. Monteiro, F. F. C. Bazito, L. J. A. Siqueira, M. C. C. Ribeiro, R. M. Torresi, *J. Phys. Chem. B* **2008**, *112*, 2102-2109.
[29] Y. Umebayashi, T. Mitsugi, S. Fukuda, T. Fujimori, K. Fujii, R. Kanzaki, M. Takeuchi, S.-I. Ishiguro, *J. Phys. Chem. B* **2007**, *111*, 13028-13032.
[30] Y. Umebayashi, S. Mori, K. Fujii, S. Tsuzuki, S. Seki, K. Hayamizu, S.-i. Ishiguro, *J. Phys. Chem. B* **2010**, *114*, 6513-6521.
[31] K. Matsumoto, R. Hagiwara, O. Tamada, *Solid State Sci.* **2006**, *8*, 1103-1107.
[32] a) M. Herstedt, M. Smirnov, P. Johansson, M. Chami, J. Grondin, L. Servant, J. C. Lassègues, *J. Raman Spectrosc.* **2005**, *36*, 762-770; b) M. Herstedt, W. A. Henderson, M. Smirnov, L. Ducasse, L. Servant, D. Talaga, J. C. Lassègues, *J. Mol. Struct.* **2006**, *783*, 145-156.
[33] C. C. Pye, W. W. Rudolph, *J. Phys. Chem. A* **1998**, *102*, 9933-9943.
[34] Rigaku corporation, **RAPID AUTO, version 2.40, (2006), Tokyo, Japan**.
[35] M. C. Burla, R. Caliandro, M. Camalli, B. Carrozzini, G. L. Cascarano, L. De Caro, C. Giacovazzo, G. Polidori, D. Siliqi, R. Spagna, *J. Appl. Crystallogr.* **2007**, *40*, 609-613.
[36] M. C. Burla, R. Caliandro, B. Carrozzini, G. L. Cascarano, C. Cuocci, C. Giacovazzo, M. Mallamo, A. Mazzone, G. Polidori, *J. Appl. Crystallogr.* **2015**, *48*, 306-309.
[37] G. Sheldrick, *Acta Crystallogr. Sect. C* **2015**, *71*, 3-8.
[38] L. J. Farrugia, *J. Appl. Crystallogr.* **2012**, *45*, 849-854.
[39] L. J. Farrugia, *J. Appl. Crystallogr.* **1997**, *30*, 565-565.